INVESTIGATION OF WATER DROPLET COALESCENCE

by
C. H. HENDRICKS
R. G. SEMONIN

Final Report
U. S. Army Material Command
U. S. Army Electronics Material Agency
Grant No. DA-AMC-36-039-63-G2
ARPA Order No. 265-62
ARPA Project Code No. 8900
Amount of Grant: $48,000
Grantee: University of Illinois

Grant Period
1 November 1962 to 31 October 1963

CHARGED PARTICLE RESEARCH LABORATORY
REPORT NO. CPRL-2-64
ILLINOIS STATE WATER SURVEY AND
DEPARTMENT OF ELECTRICAL ENGINEERING
UNIVERSITY OF ILLINOIS
URBANA, ILLINOIS

INVESTIGATION OF WATER DROPLET COALESCENCE

by

C. D. Hendricks

R. G. Semonin

Final Report

U.S. Army Material Command
U.S. Army Electronics Material Agency
Grant No. DA-AMC-36-039-63-G2
ARPA Order No. 265-62
ARPA Project Code No. 8900
Amount of Grant: $48,000
Grantee: University of Illinois

GRANT PERIOD

1 November 1962 to October 31, 1963

Charged Particle Research Laboratory
Report No. CPRL-2-64
Illinois State Water Survey and
Department of Electrical Engineering
University of Illinois
Urbana, Illinois

TABLE OF CONTENTS

ACKNOWLEDGEMENT

The project directors wish to thank Dr. H. Weickmann, U. S. Army Electronics Research and Development Laboratories, for his continued interest in the research throughout the project. The directors also wish to express their gratitude to Messrs. N. Lindblad, H. Plumlee, and E. Hassler who performed much of the work reported herein.

We gratefully acknowledge the administrative assistance of Mr. G. E. Stout, Head, Meteorology Section, Illinois State Water Survey.

Credit is also due to Mr. E. Hodges for his design of some of the experimental apparatus, and Mr. L. Lewis who prepared the drawings for this report.

Time on the IBM 7094-1401 digital computer system was made available by the Digital Computer Laboratory (partially supported by a grant from the National Science Foundation, NSFGP 700) at the University of Illinois.

ABSTRACT

The coalescence of two colliding water drops was studied by determining the surface deformation of the half-drops before coalescence in a controlled atmosphere. The surface deformation and delay time before coalescence were determined at two impact velocities, at approximately zero, 50 and 97 percent relative humidity, and at an ambient temperature of approximately 27°C. The experimental results indicate that the delay time before coalescence increases with higher humidities in both the slow and rapid collisions. At the same humidity and temperature the delay time is less in the slow collision than in the rapid collision. An electric potential difference between the drops decreases the delay time in coalescence and greatly affects the surface deformation.

To obtain quantitative results of the influence of a potential difference between two colliding drops, the time between the initial contact of two drops and their coalescence has been measured. As the potential difference was increased, this time difference was reduced. The coalescence time was 0.4 msec. for 10 volts difference compared with 4.3 msec. for 1 volt difference. Also to investigate the possibility of a charge transfer between two such drops before coalescence, the time between the initial charge flow and the coalescence of the two drops was measured. For a potential difference of 4 volts the time interval was measured to be 0.49 msec.

Most of the collision efficiencies and trajectories have been calculated for uncharged cloud droplets falling in field-free space and then in an electric field varying in intensity up to 3600 V/cm. Collision efficiencies have been determined for droplets ranging in radius from 30μ to 50μ in collision with droplets ranging from 5μ to 15μ in radius. Calculations are given to show the effects of the orientation of the electric field with respect to the axis of motion. Collision efficiencies are also given for selected pairs of droplets in extremely intense fields (10,000 V/cm).

INTRODUCTION

Theoretical calculations by Best (1951) show that the condensation process is very inefficient for producing drops large enough to be released from clouds as precipitation particles. The growth of a drop by this process is so slow that as a particle acquires a reasonable terminal velocity it will be removed from the cloud and the rate of removal will exceed the rate of formation resulting in the dissipation of the cloud. Therefore, as pointed out by Mason (1957), the condensation of water vapor alone cannot account for observed precipitation at the surface of the earth.

A more adequate physical explanation of the formation of precipitation was given earlier by Bergeron (1935) which required the co-existence of sub-cooled water droplets and ice crystals within a cloud. Bergeron's hypothesis was supported by observations of the temperatures of cloud summits made by Findeisen (1939).

The water vapor from the sub-cooled droplets will diffuse to the ice crystal by the difference in vapor pressure of ice and water at below freezing temperatures. The vapor pressure continually adjusts to a balance between the saturation vapor pressure over the ice and over the water. The vapor pressure difference results in the evaporation of the liquid droplets and the growth of the ice crystals. An assessment of precipitation processes by Houghton (1950) shows that under optimum conditions of a saturated atmosphere with respect to water at $-10^{\circ}C$, and with dendritic crystals, the formation of ice with equivalent drop size of 1.2 mm can occur. However, Houghton further states that under more typical conditions it is unlikely that drops larger than approximately 0.8 mm will be formed. Therefore, to obtain a more efficient precipitation mechanism another process must be considered, even though the Bergeron process may be more important in the initial stages of the particle growth.

In addition to the search for a more general explanation of the formation of precipitation, many observations of precipitating clouds in tropical regions, the tops of which never penetrated the freezing level, required the formulation of a theory that did not necessitate the co-existance of water droplets and ice crystals. Findeisen (1939) calculated that droplets could grow to raindrop size by falling through a sufficient depth of cloud and collecting all the droplets in the path of the larger drop. However, he did not accept his own calculations thinking they were opposed to observations. With the publication of a paper dealing with the collection efficiencies of drops of a given size by Langmuir and Blodgett (1946), it was shown that precipitation size particles could result from the cellection of smaller droplets by a larger drop introduced in the upper portions of a cloud and allowed to fall through a prescribed distribution of smaller droplets.

The study of the all-water process of precipitation formation has led to the concepts of collision, coalescence, and collection efficiencies between droplets of varying size. The collision efficiency is defined as the ratio of the area from which droplets will collide to the cross-section area of the target drop. The coalescence efficiency is the percentage of colliding droplets which merge to form a larger drop. The collection efficiency is the product of the collision and coalescence efficiencies.

One method of attempting to modify the droplet distribution within all-water clouds is to maximize these efficiencies. By the very definition of the coalescence efficiency, it can never exceed but may acquire any value less than or equal to unity. On the other hand, the collision efficiency theoretically, is unlimited. The collision between a pair of droplets is determined by the trajectories of the droplets while subjected to gravitational

and hydrodynamical forces. If additional action-at-distance forces are present or introduced, a modification of the hydrodynamic collision efficiency will result.

Thus, the problem lends itself to two, essentially independent avenues of research. On the one hand, the forces necessary to alter the relative trajectory of a droplet pair must be investigated and on the other hand the microphysics of the droplet surfaces must be studied to assure a maximum coalescence efficiency. The work reported here is an attempt to evaluate some of the possible forces and surface phenomena attendent to the maximization of the collection efficiency of water droplets.

High speed photographs of colliding drops and of the optical interference patterns formed at their boundary have been obtained under various environmental conditions. An analysis of the Newton ring patterns has shown the dependence of coalescence on the relative humidity as well as on voltages applied between the drops. These experiments permit the definition of a coalescence time or the time between visual collision and coalescence.

Further laboratory investigations on the nature of the coalescence process were carried out by photographing the profile of two colliding water drops. A small voltage was developed between the drops and the current through a series resistor was measured with an oscilloscope. The results of these data require that a more explicit definition of coalescence must be adopted.

A theoretical study of the effects of electric fields on droplet collision efficiencies is reported. The influence of an electric field is such as to always increase the collision efficiency of a droplet pair. In extremely intense fields the collision rate may be increased by orders of magnitude.

All of the work contained in this report is being extended under National Science Foundation Grant GP-2528 which will lead to a more complete knowledge of the microphysics of colliding and coalescing drops. The effects of monomolecular layers, absorbed surface contaminants, electric charge, relative velocity, and purity of the drops are a few of the subjects of future work.

The three chapters contained in this report are being prepared for submission to professional journals for publication or as partial fulfillment of the requirements for the degree of Doctor of Philosophy in the Department of Electrical Engineering. This work was presented at the National Conference on the Physics and Dynamics of Clouds, March 24-26, 1964, Chicago, Illinois.

R. G. Semonin

C. D. Hendricks

May, 1964

ILLUSTRATIONS

ILLUSTRATION (Continued)

CHAPTER I

COALESCENCE OF DISTILLED WATER DROPS

1.1 Introduction

The coalescence or non-coalescence of colliding droplets plays a significant role in various fields of research. For instance, in the growth of cloud droplets into raindrops, it is important to know some of the factors which affect the probability of coalescence of two or more colliding drops.

In this experiment the collision of two water drops was studied under quasi-static and dynamic conditions. In the quasi-static case the drops were forced together very slowly and in the dynamic case the drops were "rammed" together at two impact velocities.

The delay time before coalescence and the surface deformation of two colliding water drops (half-drops) were studied by photographing the changing interference patterns with a Fastax camera at approximately 5000 frames per second. Hereafter the half-drops will be referred to as drops. The effect of relative humidity on the delay time before coalescence was determined at approximately zero, 50 and 97 percent, and at two impact velocities. An exponential decrease in delay time was obtained by varying the potential difference between the drops from zero to 1 volt. The surface deformation at the drop surfaces was determined from the interference pattern at an applied voltage of zero, 0.6 and 0.8 volts.

Prokhorov (1954) studied the coalescence of two liquid half-drops during stationary contact in a controlled atmosphere. His results indicated that saturating the atmosphere surrounding the drops with the vapors of the same liquid was favorable for their coalescence, and that a deficit hindered their coalescence. With a deficit he found that a stable air-vapor gap or dimple

would form between the drops and remain stable for an unlimited period of time. The shape of the dimple (i.e., its thickness and width) was measured by photomicrography of the optical interference bands. If the thickness and width of the dimple did not change for a static position of the drops, the dimple was assumed to be stable. However, all the liquids examined had much higher vapor pressures than water has (Table 1). In reports of his investigation of colliding water drops, Prokhorov states: "... the forces able to preclude the coalescence of drops under static conditions plays a similar, though not so decisive, part during collision."

1.2 Experimental Methods

The drops were formed in the drop chamber on two vertical brass tubes having an inside diameter of 5 mm whose ends were separated by 1.05 mm. The cylindrical brass drop chamber was 7 cm in length and diameter. A coarse adjustment was used to bring the drops into proximity and two fine adjustments were used to move the drops slowly together. One of the latter adjustment was ultrafine and was used to investigate the stability of the dimple (air-vapor gap) in the quasi-static case. With the ultrafine adjustment the surface separation could be regulated on the order to several wavelengths of visible light. A schematic diagram of the experimental apparatus is shown in Fig. 1. In the dynamic case a pulley driven by a constant 10 rpm electric motor was used to vary the coarse adjustment to produce the slow and rapid collisions. The motor was synchronized with an event timer on the camera in such a way that when the drops were ready to collide the camera was started. The film was marked with both 60 - and 1000-cycle timing light pulses in order to establish an accurate time scale. The relative humidity of the air (mixture of nitrogen and water vapor) was

TABLE 1

Vapor Pressure of Various Liquids at 20°C

Liquid	Vapor Pressure in mm. of Hg
ether	443.4
pentane	420.2
hexane	120.0
water	17.5

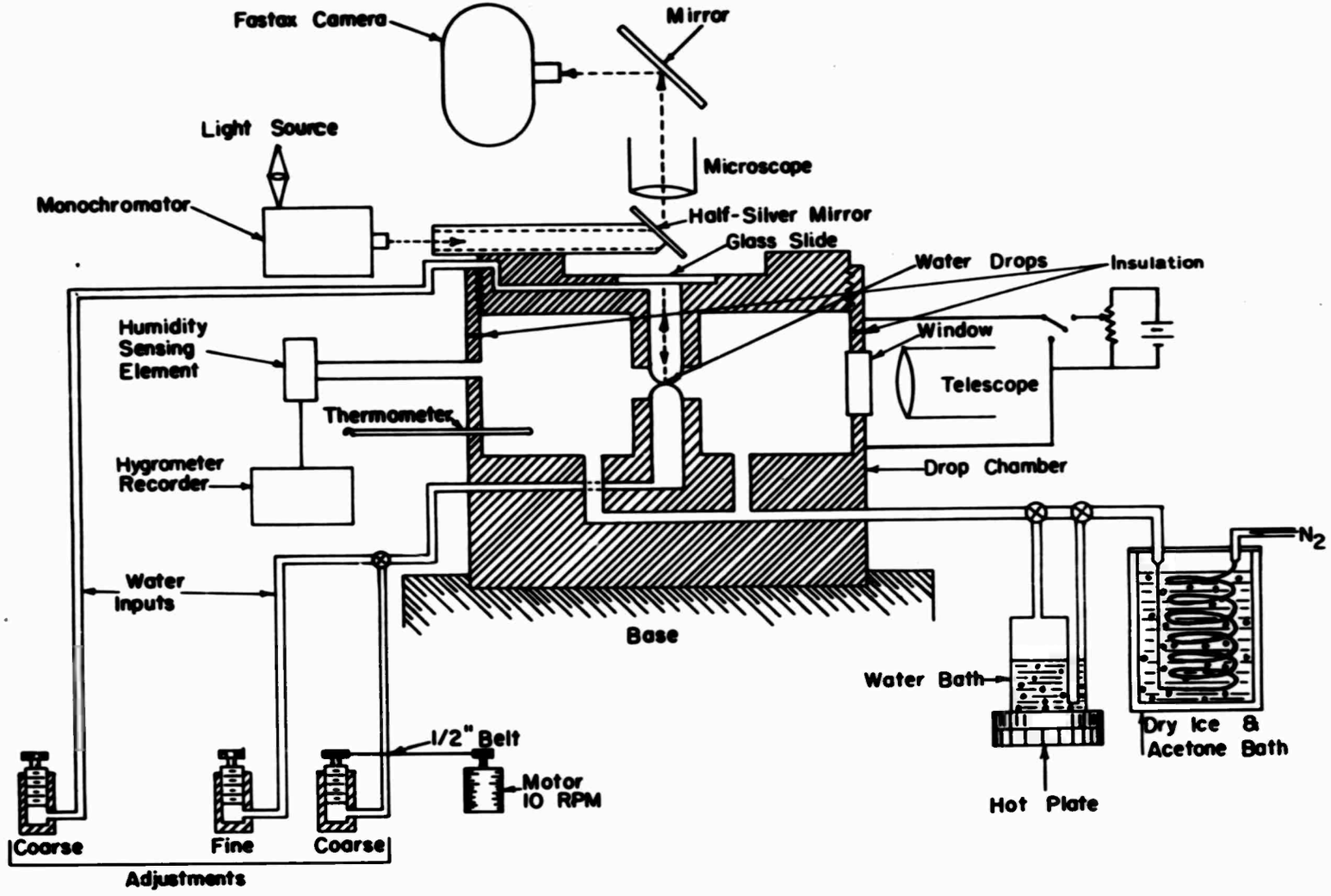

Fig. 1. Schematic Diagram of Experimental Apparatus for the Coalescence of Colliding Water Drops.

measured with a hygrometer after the air passed through the drop chamber. The sensing element had a calibration accuracy of $\pm$ 1.5 percent relative humidity. A mercurial thermometer inserted in the chamber measured the temperature. Before the dry nitrogen flowed into the chamber it was passed through copper tubing immersed in an acetone and dry-ice bath to lower the gas temperature. The desired humidity was then obtained by bubbling the dry nitrogen through water. The air-vapor gap (dimple) between the drops was illuminated with monochromatic light and the interference patterns occurring in a collision were magnified and photographed with a Fastax camera.

The following technique was used in the quasi-static experiment to investigate the stability of the air-vapor gap between the two drops. First, the relative humidity in the drop chamber was fixed by admitting the appropriate mixture of dry nitrogen and water vapor. Then the upper drop was forced out of the vertical tube so that it was halfway between the tubes. To avoid vibrating the drops, the flow of nitrogen into the drop chamber was turned off before the bottom drop was formed with the coarse adjustment. Then, the ultrafine adjustment was used to collide the bottom drop with the top drop. In this case, the interference patterns were observed through a 56-power microscope.

In the dynamic case, a motor was used to vary the coarse adjustment to move the drops together, and the different impact velocities (i.e., slow and rapid collisions) were obtained by using different pulleys on the motor. The impact velocity in the slow collision was 0.076 mm/second, and in the rapid collision it was 0.152 mm/sec. The desired relative humidity was adjusted in the drop chamber and then the top drop was formed as in the quasi-static case. Before the bottom drop was forced to collide with the top drop,

the flow of nitrogen into the drop chamber was shut off. The interference patterns resulting from the rapid and slow collisions were photographed through an objective lens with a Fastax camera.

In the slow and rapid collisions the delay time before coalescence was determined at humidities of approximately zero, 50 and 97 percent, at temperatures ranging from 25° - 29°C. The time lapse, from the start of the initial flattening of the drop surfaces until coalescence, was defined as the delay time.

1.3 Experimental Results

a) Dimple stability of water drops. The quasi-static collision of two water drops was examined to determine the existence of a stable dimple. The relative humidity in the drop chamber was varied from zero to 96 percent at a temperature of 27°C. After the top drop was formed, the bottom drop was moved upward very slowly. As the drops moved closer together, the interference patterns would suddenly appear and change very rapidly until a large bright spot appeared in the center of the pattern. The bright spot indicated that some flattening occurred before the drops coalesced. Even though this pattern was repeated many times, a stationary pattern similar to that photographed by Prokhorov could not be formed at the low or high humidities.

b) Effects of relative humidity and impact velocity on coalescence. The delay time before coalescence for the slow and rapid collisions at various relative humidities is depicted in Fig. 2. Even though the points for both the slow and rapid collisions are widely scattered, there seems to be a trend which indicates that the delay time increases with higher humidities which is contrary to Prokhorov's results. Prokhorov in his collision

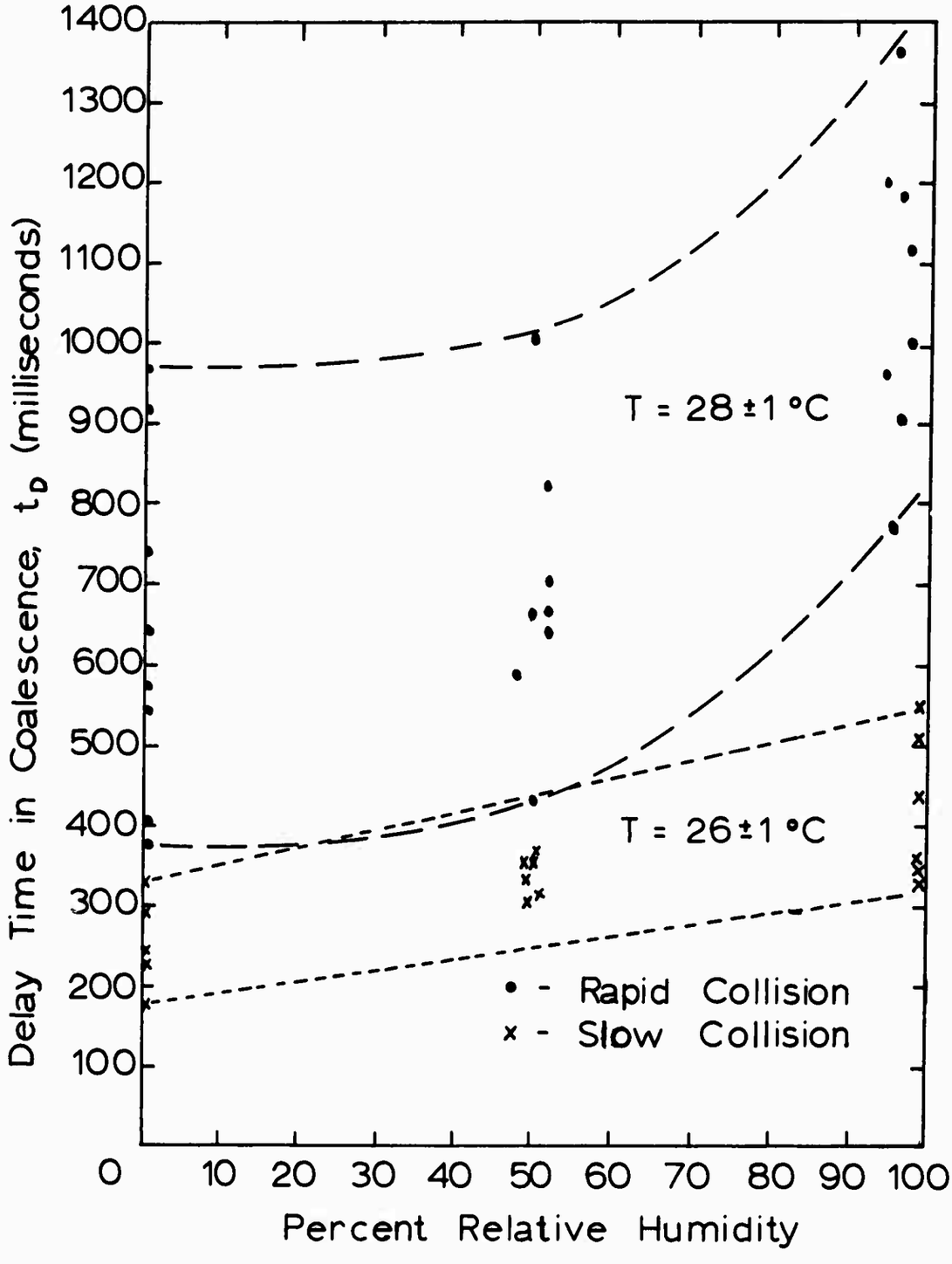

Fig. 2. Delay time in coalescence of slow and rapid colliding water drops at various humidities.

experiment had one drop (hemisphere of water) projected out of a lower capillary and the other drop (top drop) was forced out of the upper capillary and allowed to fall and collide with the lower drop. The collisions were carried out at relative humidities of 20, 75 and 100 percent. By displacing the lower drop in a horizontal plane he determined a coalescence zone which increased with relative humidity. This result indicates that the colliding drops coalesce more readily at the higher humidities. Figure 2 also shows that the impact velocity is as important as the percent of relative humidity in determining delay times, as evidenced by the shorter delay times occurring for the slow collisions.

c) Interference patterns for colliding water drops. A few photographs showing the interference patterns for two rapidly colliding water drops at zero relative humidity and 27°C are shown in Fig. 3. The photographs were retouched because of the difficulty in exposing the film with monochromatic light at 5000 frames per second. A profile of the drop surfaces is indicated beneath each interference pattern.

The central dark spot in the interference pattern in Fig. 3a indicates the start of the initial flattening. The dark spot grew wider for 14.5 msec. with no change in the minimum surface separation. Then the center of the dark spot started to brighten, indicating an unflattening of the surfaces. The bright spot grew into the central bright spot in Fig. 3b, which shows the second stage of flattening. This spot widened for 31 msec. with no change in the minimum surface separation. The initial formation of the dimple started with the appearance of a grey band (not shown in a photograph) inside the bright spot shown in Fig. 3b at a radial distance of 0.25 mm. from the center. The appearance of the grey band indicates that the surface separation

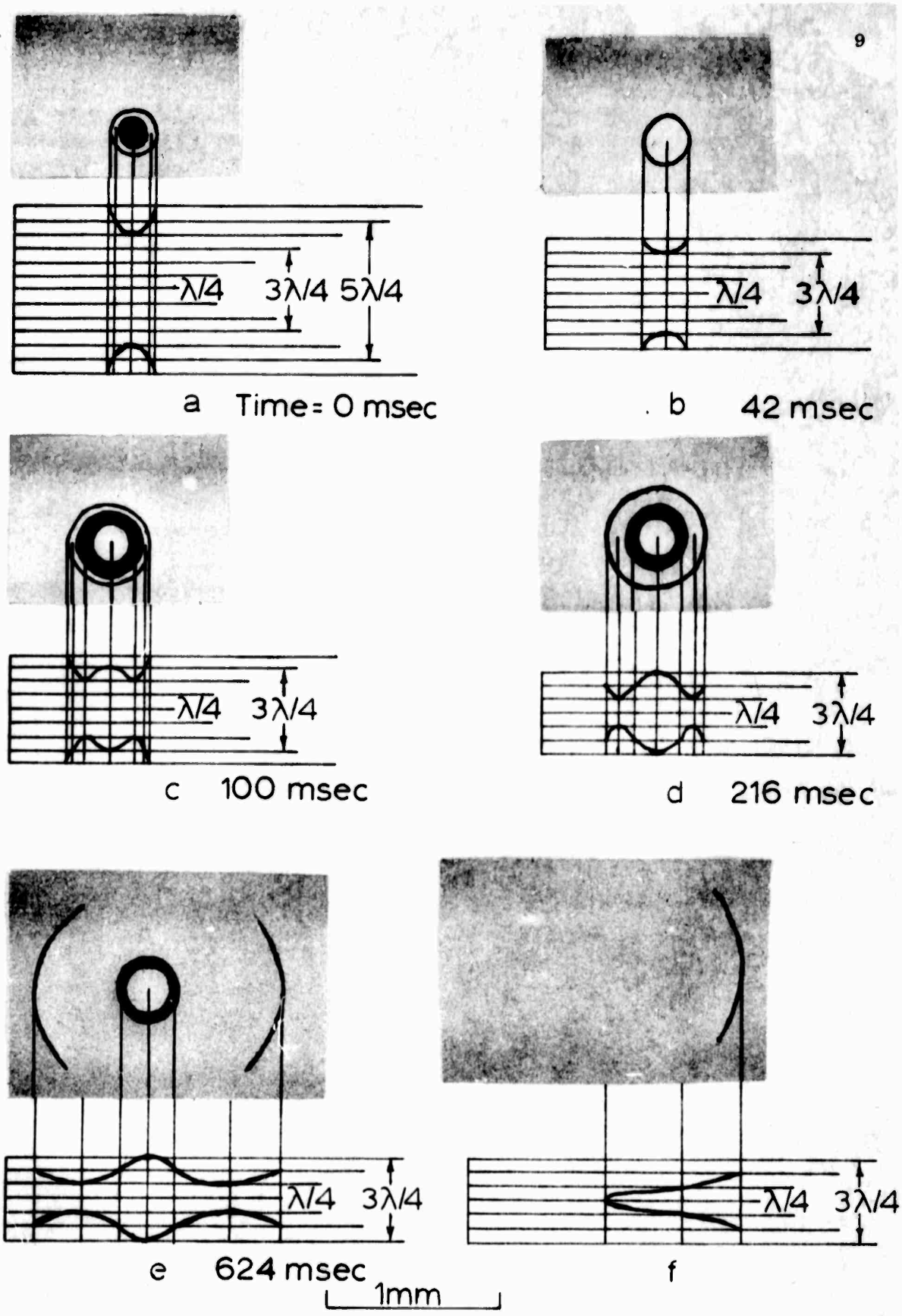

Fig. 3. Interference patterns and drop surface profiles for rapidly colliding distilled water drops.

has started to decrease. Observations made by Allan, et. al. (1961) on the approach of gas bubbles to gas/liquid interface and Derjaguin, et.al. (1939), Elton (1948) for gas bubbles approaching a flat surface have also shown the minimum separation is no longer at the center of the interference pattern, but along a circle at a radial distance, r, from the center. The grey band developed into the first dark band shown in Fig. 3c, which indicates the first dimple stage. The width of the interference pattern grew for 90 msec. before deepening of the dimple started. Fig. 3d shows the deepening of the dimple with the appearance of the first bright band. This band appeared inside the first dark band shown in Fig. 3c, i.e., it split the dark band in Fig. 3c into the first and second dark band shown in Fig. 3d. Figure 3e is the last frame before coalescence and the profile of the drop surfaces indicates the final form of the dimple. Note how the thin second bright band in Fig. 3d has grown into the wide second bright band in Fig. 3e. This indicates that the drop surfaces are extremely flat at the minimum separation. Figure 3e also shows that the central separation has not changed since the second flattening of the drop surfaces. The second dimple stage lasted for 433 msec. Figure 3f is the frame after the one shown in Fig. 3e and indicates the coalescence started sometime between Fig. 3e and Fig. 3f. The remaining faint bands in the latter figure show that coalescence started on the left side of the dimple and has proceeded approximately three-quarters of the way across. The horizontal scale is indicated at the bottom of Fig. 3.

To determine the thickness of the gap it was assumed that the surfaces would have to be almost touching for coalescence to occur, i.e., the surface separation should be less than $\lambda/4n$. For the above case λ = 5800 Å. and n is the index of refraction of the medium between the two drops. A good approximation

for n is unity. Therefore, the minimum surface separation was 1450 Å. which corresponds to about 600 molecular diameters. On a molecular scale such a surface separation is still large, so that one would expect coalescence to occur when the surface separation is less than $\lambda/4$. The experimental evidence to support the latter statement is obtained from Fig. 3f where it is seen that coalescence has proceeded over more than half of the surfaces. In this case, the profile of the drop surfaces looks like a wedge with no interference bands between the center of the interference pattern and the points of minimum separation. From this it is concluded that the minimum separation must be $\lambda/4$. For instance, if the minimum separation was $3\lambda/4$, then between the center and the points of minimum separation there would be a bright band corresponding to $\lambda/4$ and a dark band corresponding to $\lambda/2$. One might expect with the presence of a dimple that air and the vapor could be trapped in the liquid after coalescence. However, as illustrated in Fig. 3f, coalescence started on the side of the dimple, probably at the minimum separation, and then proceeded rapidly across, forcing out the trapped air and vapor. Coalescence of the two drops was assumed to have been completed upon the disappearance of the interference bands.

To determine the average coalescence time for rapidly colliding drops at zero percent humidity and 27°C, the drop surfaces were illuminated with white light from a d-c carbon-arc lamp. The latter time was measured from the start of the disappearance of the Newton rings to complete disappearance. In this case, the film speed was 14,500 frames per second. An examination of five collisions gave an average coalescence time of 0.21 ± 0.07 msec.

In Fig. 4 the minimum surface separation was plotted versus time to indicate the different stages in the surface deformation of the two drops. The interference pattern in Fig. 3a corresponds to the region of first

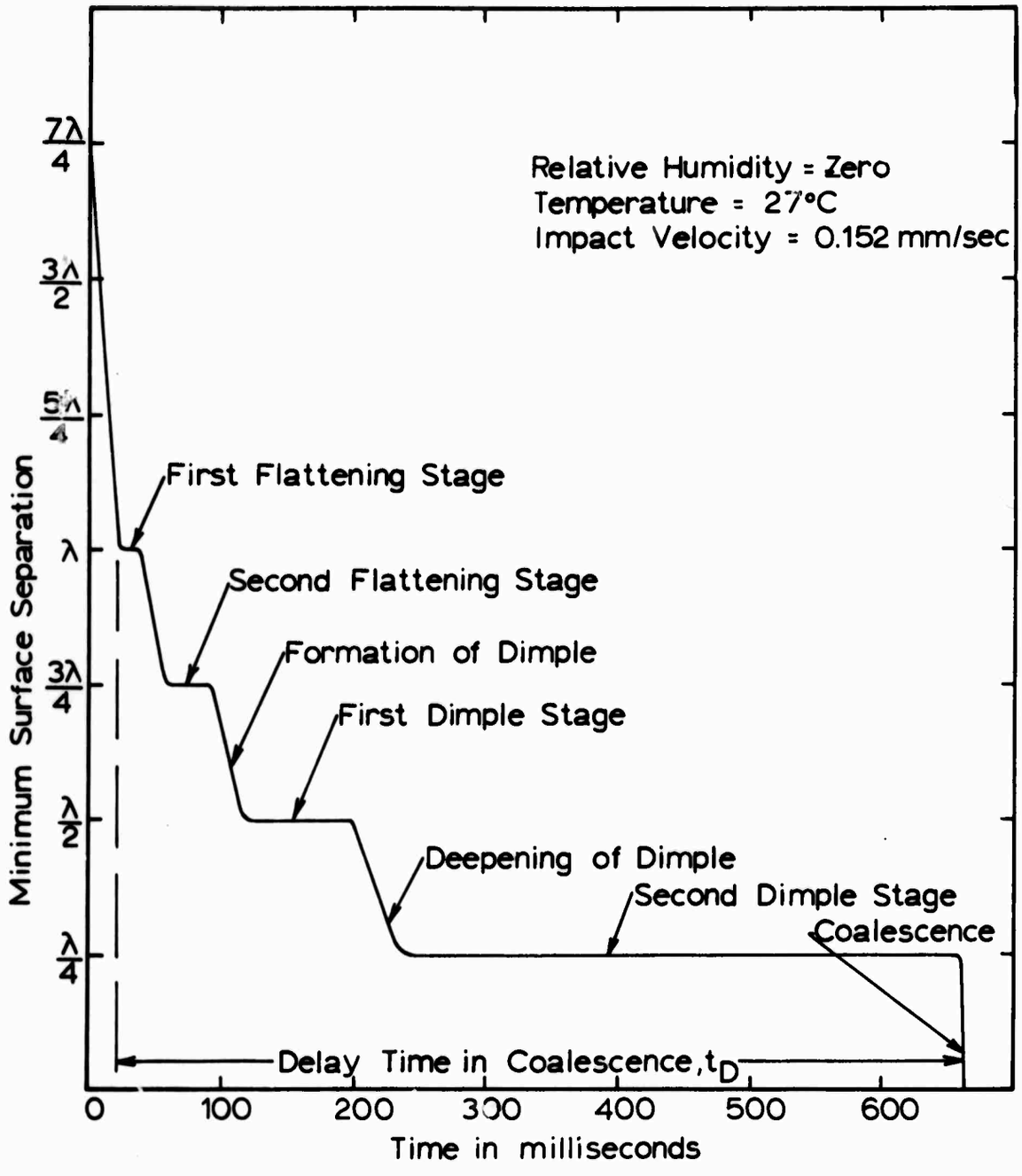

Fig. 4. Surface deformation at different stages for two rapidly colliding water drops.

flattening shown in Fig. 4, Fig. 3b, to the second flattening, Fig. 3c to the first dimple stage, Fig. 3d and 3e to the second dimple stage. The difference between the curve shown in Fig. 4 and those reported by (2, 5) is the plateau regions during which the minimum surface separation did not change and only the interference patterns grew in width.

The presence of a central maximum separation and a minimum separation is a characteristic feature of all the colliding drops examined, except water drops forced to collide in an Octoil (2 - ethylhexyl phthalate) medium. This latter experiment is discussed below.

d) Retardation of water drop evaporation. To examine the possible effects of evaporation rate on dimple formation, the water drops were forced together in an immiscible medium of Octoil. In this case, the drop surfaces flattened without any sign of dimpling. The drops could be maintained in contact for as long as five minutes without coalescence. Varying the impact velocity had no effect on coalescence delay time except on the rate of flattening, i.e., the rate of flattening of the drop surfaces occurred more rapidly in the rapid collision. This seems to indicate that dimple formation is dependent upon the evaporation rate. To obtain more conclusive evidence, the surface deformation of colliding drops with very low vapor pressure was studied. For colliding Octoil drops (rapid collision) the drop surfaces first flattened and then dimpled. The dimple started to disappear approximately 0.42 ± 0.14 msec. before the start of coalescence, i.e., the drop surfaces started to reflatten. Coalescence time was 0.56 ± 0.14 msec. The delay time for the colliding Octoil drops in air at zero humidity and 25°C was 1.25 sec. At 20°C, Octoil has a vapor pressure of approximately 10^{-8} cm. of Hg.

A mixture of hexadecanol and octadecanol in an emulsion was placed on the two water drops and allowed to spread to form a multilayer. A long-chain alcohol mixture was used because of its ability to retard the rate of evaporation of water. (Geoffrey, et.al., 1962). In the slow collision case the drop surfaces first flatten and then dimpled, but the delay time was approximately 600 msec., which is a typical delay time for the rapid collision range without a multilayer. The temperature of the ambient air was 27°C and the relative humidity, zero.

e) Electrical effects of dimpling. The delay time, for two uncharged drops forced to coalesce, varies over a wide range as indicated in Fig. 2. However, when an electrical potential difference is applied between the drops, the scattering of points is greatly reduced, as shown in Fig. 5. The latter figure also shows that there is a converging of scattered points as the potential difference is increased. It is obvious that there is a reduction in delay time with an increase in potential difference. This latter result was also reported by Berg (1963).

The photographs shown in Figs. 6 and 7 indicate the effect of electrical forces in the narrow gap (dimple) between the drop surfaces. In Fig. 6c the two small bright areas indicate that a small pointed projection has formed on the surface of the drops. Since the region where the pointed projection is formed changes from dark to bright, the surface separation must be $\lambda/4$. The height of the projection may be either $\lambda/4$ or $\lambda/8$, depending on whether the projection was formed on both or just one of the surfaces. In all cases where the drops were uncharged, the depth of the dimple was $\lambda/4$ before coalescence. However, when the drops are charged the depth of the dimple can be greatly affected. Figure 7j shows a dimple depth of $3\lambda/4$ when a potential difference of 0.6 volts was applied.

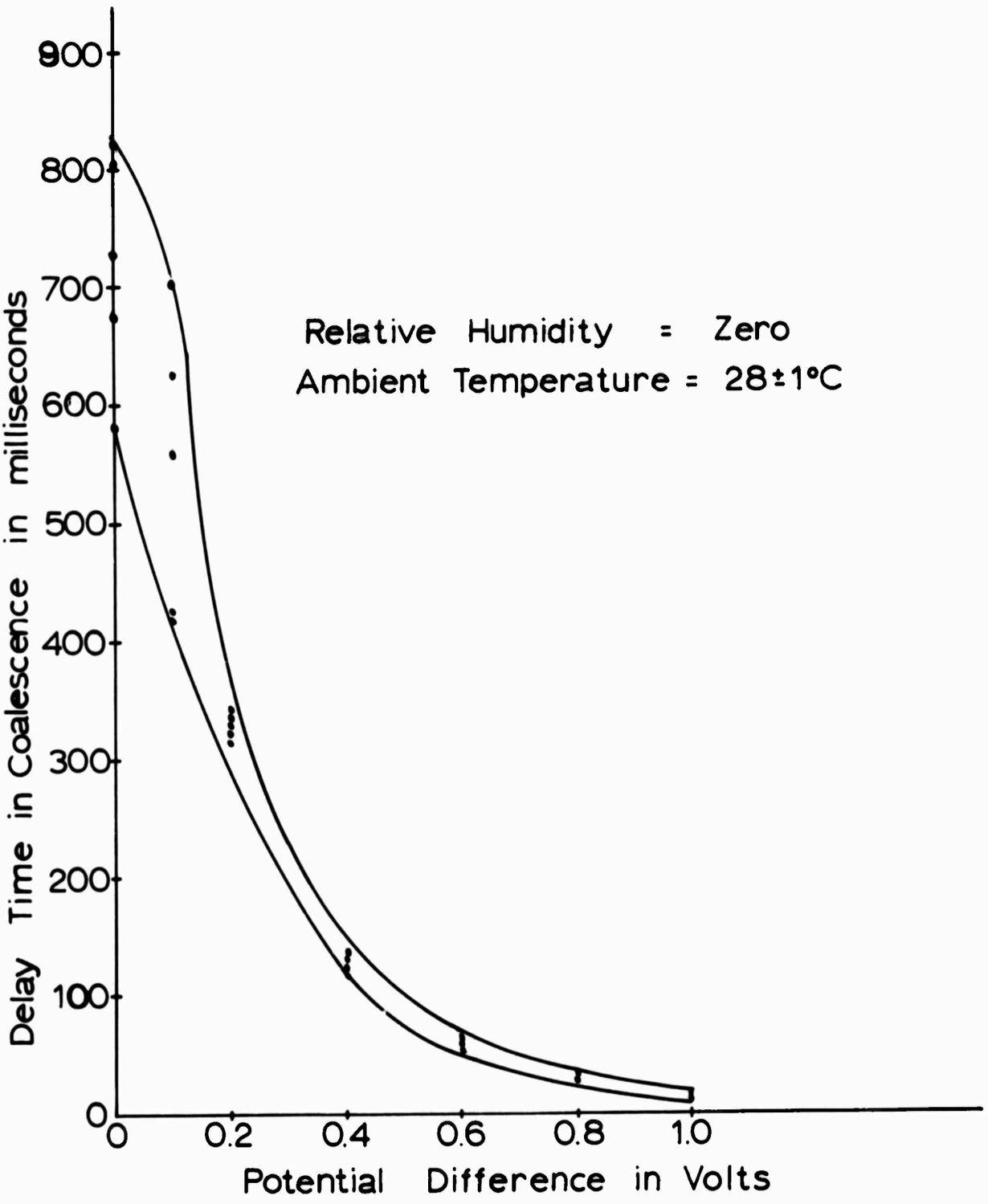

Fig. 5. The delay time in coalescence as a function of potential difference for rapidly colliding distilled water drops.

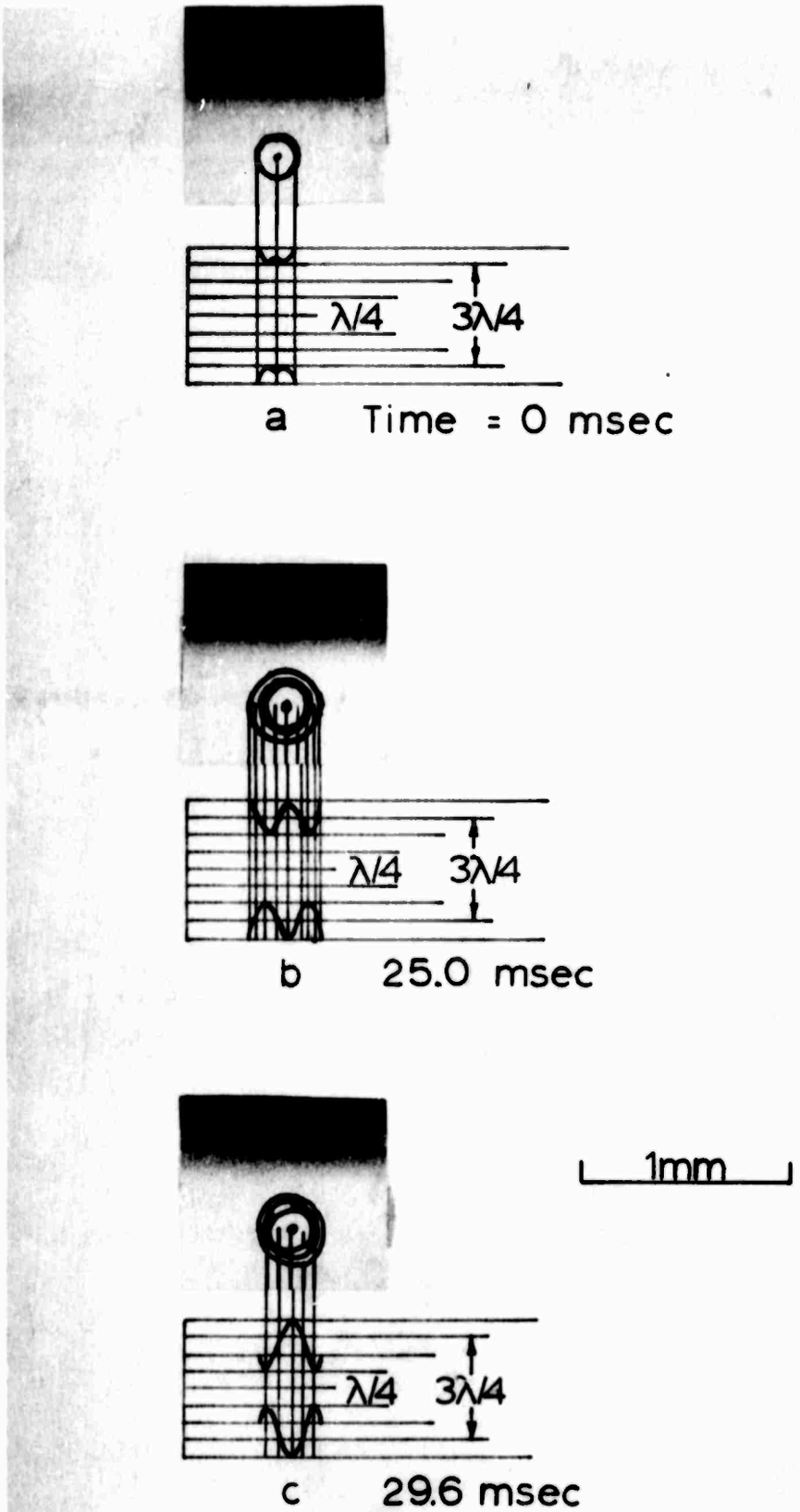

Fig. 6. Interference patterns and drop surface profiles for rapidly colliding distilled water drops with a potential difference of 0.8 volts.

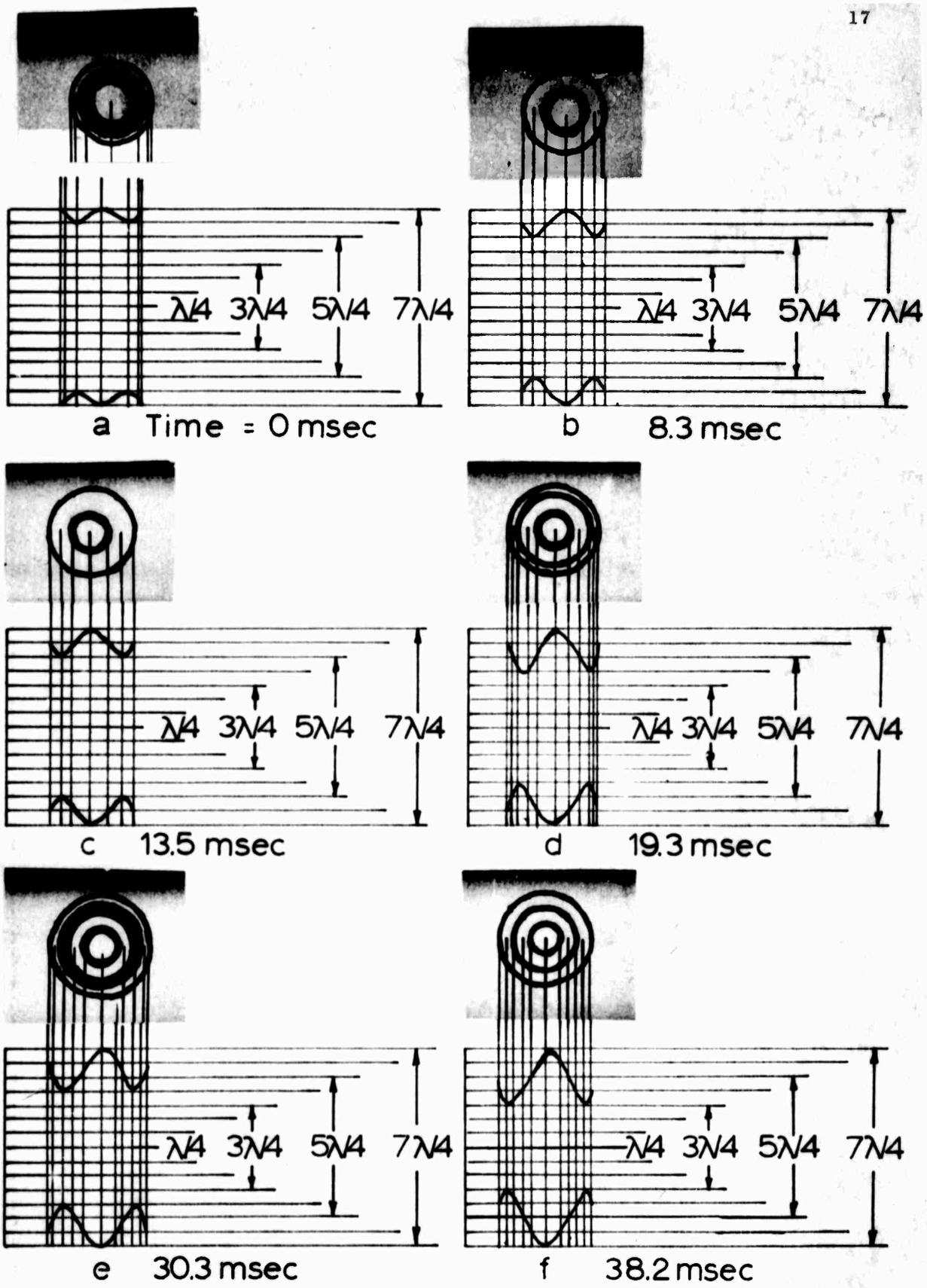

Fig. 7. a-f. Interference patterns and drop surface profiles for rapidly colliding distilled water drops with a potential difference of 0.6 volts.

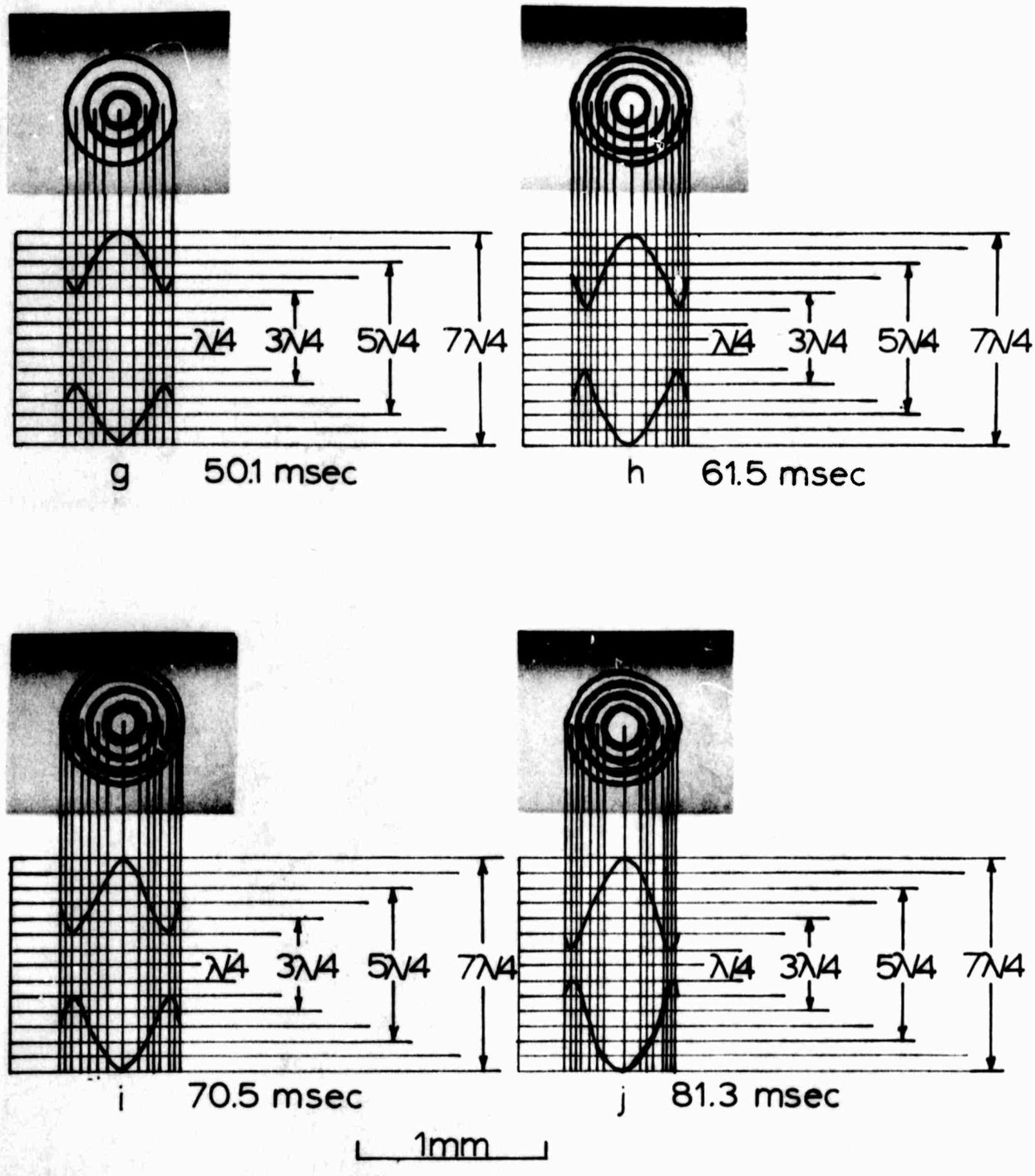

Fig. 7. g-j. Interference patterns and drop surface profiles for rapidly colliding distilled water drops with a potential difference of 0.6 volts.

1.4 Discussion

a) Stable and unstable air-vapor gaps. The experimental difficulty encountered in the quasi-static case in obtaining a stable gap between water drops indicates that a stable gap may be a property of liquids possessing vapor pressures higher than for water. For a qualitative discussion we will assume that dimpling depends on the drop evaporation rate and the molecular flow out of the dimple. The initial formation of the dimple is caused by the surplus pressure due to the evaporation. Let $\underline{dN_1/dt}$ represent the number of molecules evaporating from the flattened surface per unit time, and let $\underline{dN_2/dt}$ be the total flow of molecules out of the dimple per unit time. When $\underline{dN_1/dt} > \underline{dN_2/dt}$ one would expect to have a stable dimple, and when $\underline{dN_1/dt} < \underline{dN_2/dt}$ the dimple should be unstable. Thus, for liquids with high vapor pressures (high rates of evaporation) $\underline{dN_1/dt}$ should be equal to or slightly greater than $\underline{dN_2/dt}$. Liquids falling into this class would be ones with vapor pressures greater than 100 mm. of Hg at 20°C. In the case of water, $\underline{dN_1/dt}$ is probably less than $\underline{dN_2/dt}$ since a stable gap could not be obtained. However, the water drops can be made to dimple if they are moved together faster. When the drops are moved together at higher velocities, the air and vapor between have less time to diffuse out. This is indicated by the lower delay times in the slow collision over those obtained in the rapid collision. For colliding Octoil drops the experimental results indicate $\underline{dN_1/dt}$ must be initially large enough to produce dimpling but not large enough to maintain the dimple. Since the drop surfaces reflatten, the molecular flow out of the dimple must exceed the evaporation rate into the dimple. It is only a hypothesis at this time that the dimple will either be stable or unstable as determined by the evaporation rate. More experimental and theoretical work is

needed to determine which physical parameters cause the dimpling. At present there is no satisfactory theoretical explanation for the fact that the surfaces of two colliding drops first flatten and then dimple.

b) Influence of surface contaminants and age of the distilled water. When the water drop surfaces were contaminated with a multilayer mixture of 65 percent octadecanol and 33 percent hexadecanol, the delay time in coalescence increased approximately by a factor of two. The effects of other surface contaminants on the coalescence process are being studied.

In this experiment it was noted that when fresh double-distilled water (water not exposed longer than one hour to the air) was used, the delay time was approximately half as long. The distilled water was enclosed in a polyethylene bottle opened to the air through a narrow polyethylene tube inserted in the water. The distilled water used to obtain the experimental data for this report was stored in the coarse adjustments for about 30 hours before use.

c) Delay times. The experimental results indicate that the delay time in coalescence increases slightly with relative humidity. Before two drops can coalesce most of the air and vapor between the drops must be forced out. The molecular flow per unit time out of the gap is given by $\underline{dN_2}/\underline{dt} = 1/4\ \underline{V}\ (\underline{n_1} - \underline{n_0})\ \underline{A}$ where $\underline{V}$ is the average velocity of the vapor molecules, $\underline{n_0}$ the number per cm^3 outside the dimple, $\underline{n_1}$ the number per cm^3 inside the dimple, and $\underline{A} = 2\pi\ \underline{rh}$ min. $\underline{r}$ is the radial distance from the center of the dimple to the point of minimum surface separation, $\underline{h}$ min. Thus, as the ambient relative humidity is increased, $\underline{n_0}$ increases and $\underline{dN_2}/\underline{dt}$ becomes less, which means the molecular flow out of the dimple is retarded when the relative humidity is increased. Since the molecular flow out of the dimple is retarded at higher humidities one would expect longer delay times at these humidities.

The experimental results also show that a shorter delay time occurs at a lower impact velocity. The shorter delay times are due to the fact that the fluid has a longer time to flow out between the drops. However, $\underline{dN_2/dt} = 1/4\ \underline{V}\ (\underline{n_1} - \underline{n_0})\ \underline{A}$ does not predict the effect of impact velocity on the rate of molecular flow out of gap.

The case illustrated in Fig. 3, as well as numerous others not discussed in this report, shows that the approaching drop surfaces flattened twice before the dimple was formed. For uncharged drops the dimple formation goes through two stages as shown in Fig. 4. When the drops are charged, the second stage is not always completely formed. For instance, in Fig. 6c, two pointed projections form instead of the regular bright band which corresponds to the minimum surface separation.

1.5 Summary

In the quasi-static case where the drops were moved together very slowly, a stable dimple (air-vapor gap) between two water drops was not observed at the low or high relative humidities.

The delay time before coalescence and the surface deformation were determined in the dynamic case where the drops were "rammed" together at two impact velocities. The experimental results indicate that the delay time tends to increase when the ambient relative humidity was increased. However, lower delay times were obtained in the slow collision case as compared to those in the rapid collision case. When the drop surfaces were contaminated with chemicals which retard the rate of evaporation of water, the delay time was increased approximately by a factor of two. An exponential decrease in the delay time was obtained when a potential difference between the drops was varied between zero and one volt. At an applied voltage of 0.6 and 0.8 volts the surface deformation, such as the dimple depth, was affected greatly compared to the case when no voltage was applied.

BLANK PAGE

CHAPTER II

ELECTRICAL EFFECTS ON THE COALESCENCE OF PAIRS OF WATER DROPS

2.1 Introduction

The influence of electric charges and fields on the coalescence of water drops has been studied by several investigators. Rayleigh (1878) was one of the first investigators to observe the effects of such influence. He noted that a jet of water directed up into the air would produce either a spreading of the droplets formed or would collapse back onto itself, depending upon whether or not an electric field was present at the point of the jet breakup. He suggested that the spreading was due to collisions between droplets which did not coalesce. However, in the presence of an electric field, the charge on each droplet was increased which resulted in a greater number of coalescences and a reduction in the spreading of the droplets.

Levin (1954) gave some calculations which suggested that the effects of charges might materially increase the collection efficiency of two small droplets (order of 1 to 2 microns in diameter). Also in that year Sartor (1954) reported an investigation of the coalescence of drops in an electric field. He studied water drops falling through mineral oil and observed a very definite increase of collection efficiency as an applied electric field was increased. During this investigation Sartor observed several events which he attributed to the transfer of charge between two water drops on the tip of two glass fibers in the presence of an electric field. For a small initial separation of the two water surfaces, the drops moved together as the electric field was increased, then separated suddenly. With a further increase in the electric field, the drops again moved together. Since the electric field is enhanced between surfaces which are very close together,

a breakdown of the air with a charge transfer was given as a mechanism to explain these events.

Berg (1963) reported some quantitative results of the influence of a potential difference on the coalescence properties of two drops. He indicated that the time between visual contact and the coalescence of two water drops is greatly reduced as the potential difference is increased from zero to 10 volts.

In order to verify some of the earlier observations and to extend our knowledge of the coalescence process, the following study was carried out.

2.2 Experimental Technique

No satisfactory method has been found to allow careful study of two single coalescing drops freely falling in air. Therefore, it has been necessary to constrain the two drops in order to conduct an investigation. In this study, drops were formed at the tips of two number-18 hypodermic needles which were etched so the tip would be flat. One needle was mounted rigidly inside a closed, electrically shielded chamber. The second needle was mounted on pivots in such a way that the tip would swing very close to the tip of the stationary needle, permitting a collision between the drop pair. The velocity at which the drops collided was varied by changing the length of the pendulum needle.

A 16 mm Fastax camera was used to take high speed photographs of the profile view of the two colliding drops. Since the one drop was held stationary, the optical system for photography was greatly simplified. Two d-c carbon arc lamps were used to illuminate the drops. One lamp was placed slightly to the right and above the camera itself. This lamp furnished the front lighting giving a better three-dimensional appearance to the photographs.

The second lamp was placed behind the drops directly in line with the camera lens. A mylar diffusion screen was placed approximately 0.5 cm behind the drops to reduce highlights. With this arrangement, photographs at a speed of 14,000 frames per sec. were taken of the profile view of the collision and coalescence of the two drops. The sequence of events for taking these photographs was predetermined by timing clocks. The camera was started first to allow it to reach a high film velocity before the pendulum was released from a solenoid operated clamp.

The potential between the two drops was varied by electrically insulating the two needles and applying variable voltage between them. A precision 10 ohm resistor was placed in series with this circuit, as shown in Fig. 8. The current in the circuit was monitored by measuring the voltage across this resistor with one channel of a dual beam Tektronix oscilloscope, type 551. The second channel monitored the voltage applied across the two needles, and a Tektronix oscilloscope camera model C-12 was used to record these quantities. The oscilloscope was adjusted so the trace was triggered by the initiation of the current. Since the circuit was normally open, only with the coalescence of the two drops did any charge flow.

Two neon lamps were mounted in the Fastax camera in such a way that their light was recorded along the extreme edges of the 16 mm film. One lamp was used to record 1,000 cps timing pulses. It was fed by a rectangular electrical pulse of equal on and off duration. This provided a means to measure the time between different events photographed on the film. The second neon lamp was used to record the time of the initial flow of current in the electrical circuit. The lamp was turned on by a thyratron tube triggered by the initial current. A time delay of less than 20 μ sec. was measured for this triggering

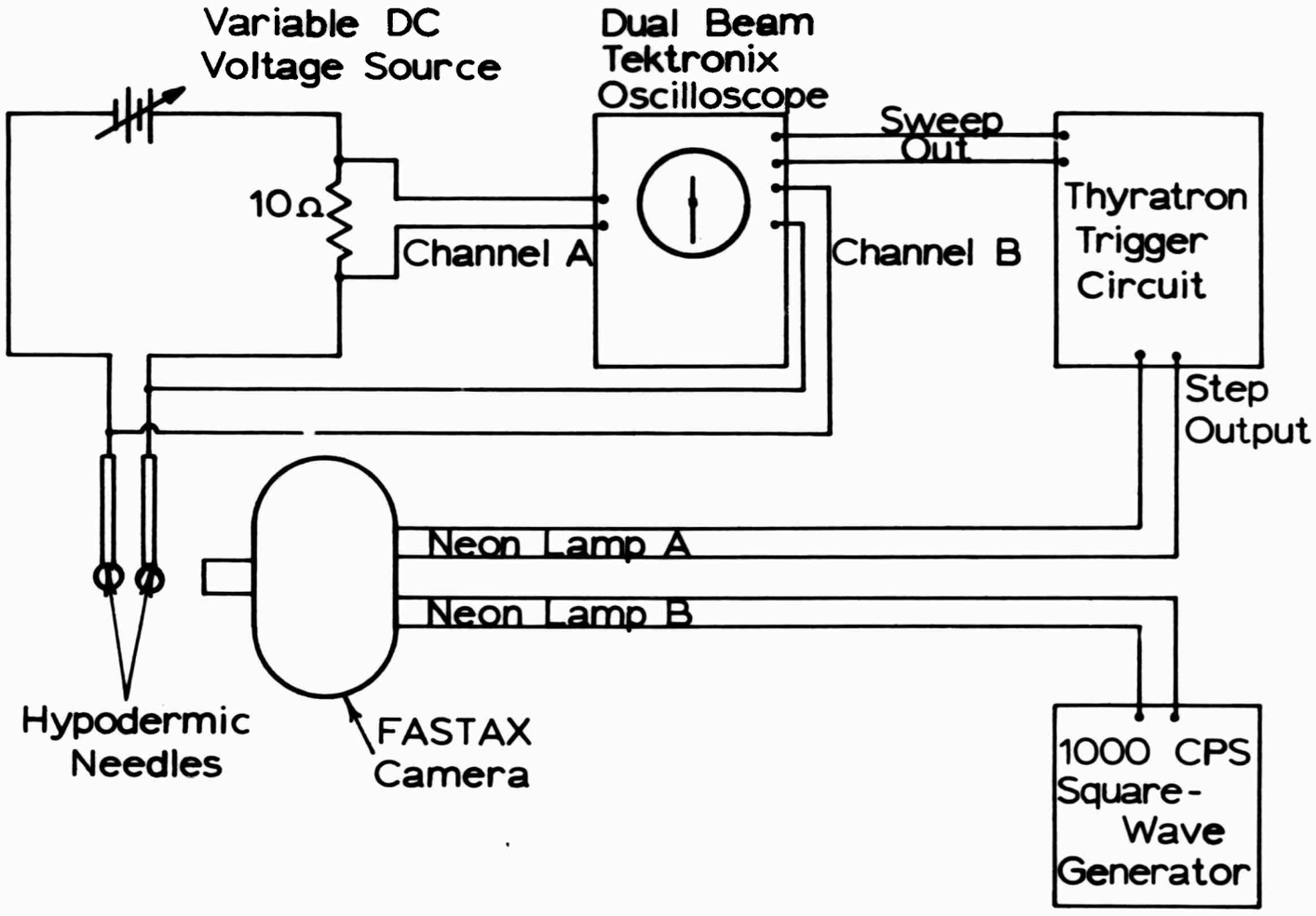

Figure 8. Block diagram of the experimental apparatus for measuring the current between colliding water drops.

circuit. This procedure provided a means to measure when the current initially started to flow relative to the events recorded on the film.

Measurements from the film were taken by the use of an analog-to-digital converter. Scaling of distances was accomplished by accurately measuring the diameter of the tip of a hypodermic needle and comparing this with its measurement from the film. The collision velocity was determined by measuring the approach of the two drop surfaces as a function of the 1000 cps timing marks along the edge of the film. After the collision of the two drops, but before their coalescence, the rate of deformation of the adjacent surfaces was determined by measuring the height of the flattened region. At coalescence a transition region between the drops was formed which has the appearance of a lens. Photographs of both the flattening and the lens are shown in Figure 9. The rate of growth of both the height and width of this lens was measured.

The initial appearance of this lens was taken as the beginning of the coalescence process. The time between the visual contact of the drop surfaces until appearance of the lens is defined as the coalescence time. The time between the initial flow of charge and the initial appearance of the lens is defined as the current time. The difference time which was easily determined within 2 frames of the film gave an accuracy of $\pm$ 150μ sec.

2.3 Experimental Results

To insure adequate current for reliable measurements distilled water with a small amount of HCl was used. This solution had a pH = 1.9 and a conductivity $\sigma = 6 \times 10^{-3}$ mhos/cm. Only two collision velocities have been used (27 cm/sec and 10 cm/sec). Both drops had a radius of approximately 2 mm. The voltage between the drops was varied between 0 and 10 volts d-c. Temperature and relative humidity were approximately 20°C and 40 percent respectively. A typical set of photographs of the collision and coalescence are shown in Figure 10.

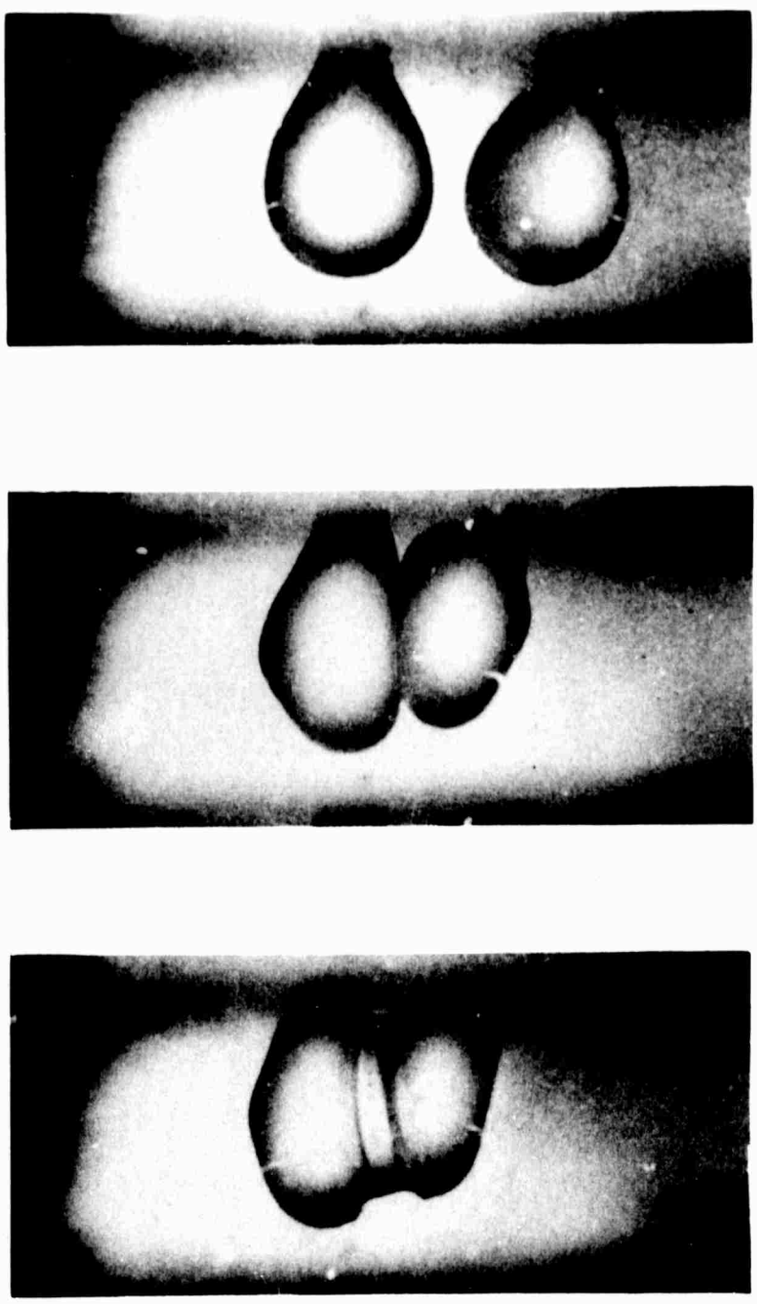

Fig. 9. Photographs showing the profile of two water drops before collision, after collision, and after coalescence.

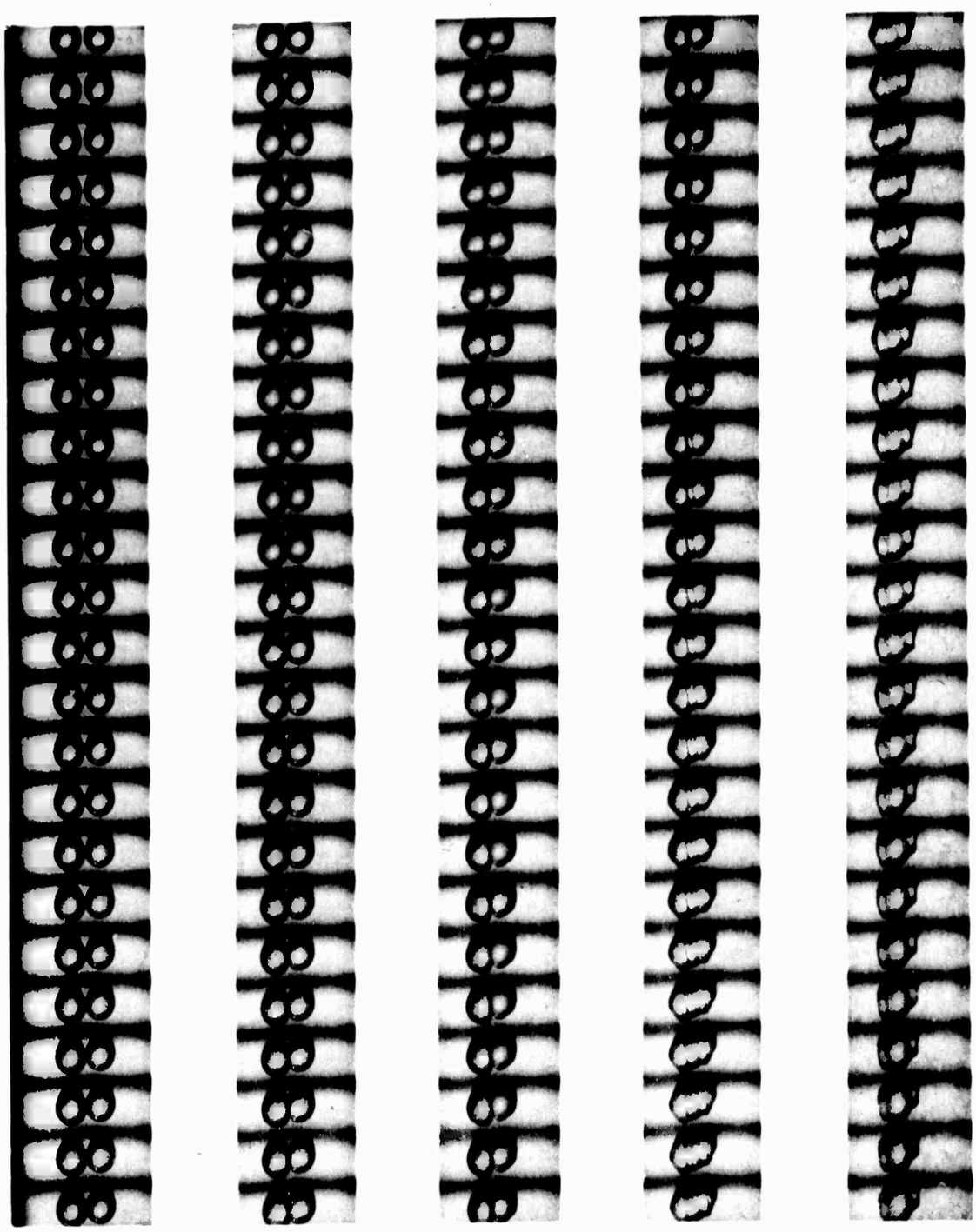

Fig. 10. A sequence of photographs taken at 14,000 frames per second of colliding and coalescing water drops with a potential difference of 1 volt.

Figure 11 is a plot of the reciprocal of the coalescence time for the two collision velocities as a function of the applied voltage. For voltages less than 1 volt the spread in the data increased and became somewhat random. This range of voltage was not investigated completely and the curves were merely projected to 0 voltage. For the range of 0-0.5 volts, a collision followed by a separation of the two drops was easily obtained by adjusting the pendulum so it would separate the drops before the minimum coalescence time. Photographs of this separation are shown in Figure 12. Figure 11 indicates that at the lower voltages, the coalescence time is inversely proportional to the applied voltage, but the slope is slightly different for different collision velocities. However, for larger applied voltages the coalescence time becomes independent of the collision velocity. The plot also shows that the coalescence time decreases as voltage is increased. For 10 volts applied, the coalescence time is 0.4 msec. compared with 4.3 msec. for 1 volt applied.

As was noted earlier, for small potential differences, the inverse of the coalescence time was linearly proportional to the voltage. Berg (1963) suggested that the formation of intermolecular bonds across the interface was achieved by a gradual rearrangement of the orientation of the electric dipoles. The force to realign the dipoles with a moment, μ , would be proportional to μE where E is the field strength. But since E is proportional to the voltage, V, the realigning force would be proportional μ V. However, if the voltage is increased above a certain value, the inverse of the coalescence time becomes proportional to the square of the voltage as shown in Figure 13. This may be the result of the breaking of old bonds and the making of new bonds. Since the drops act as a capacitor of capacitance, C, they would have an energy supply of $1/2\ CV^2$. The discharge of this energy might favor the breaking of bonds.

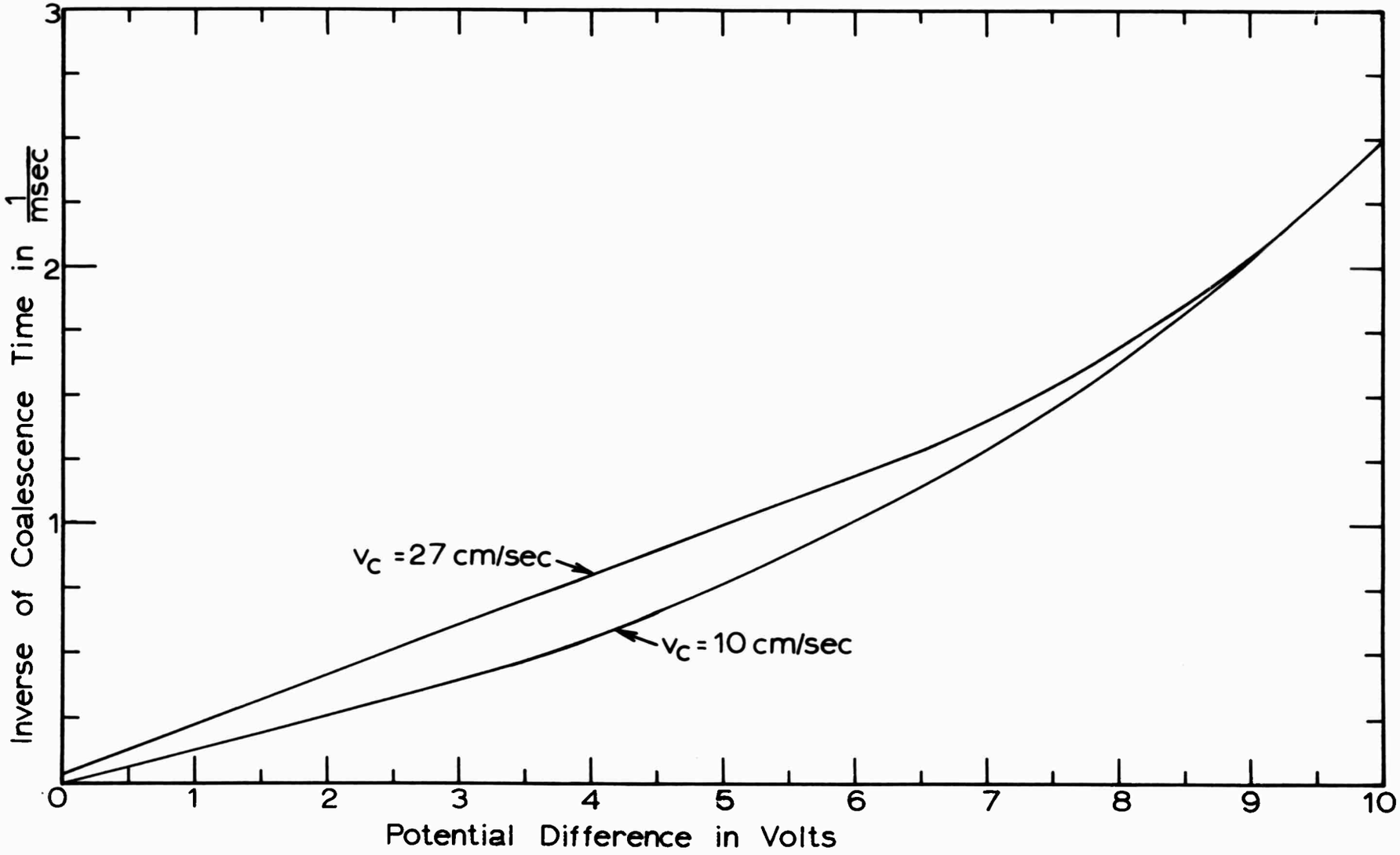

Fig. 11. A plot of the inverse of coalescence time as a function of the potential difference between drops.

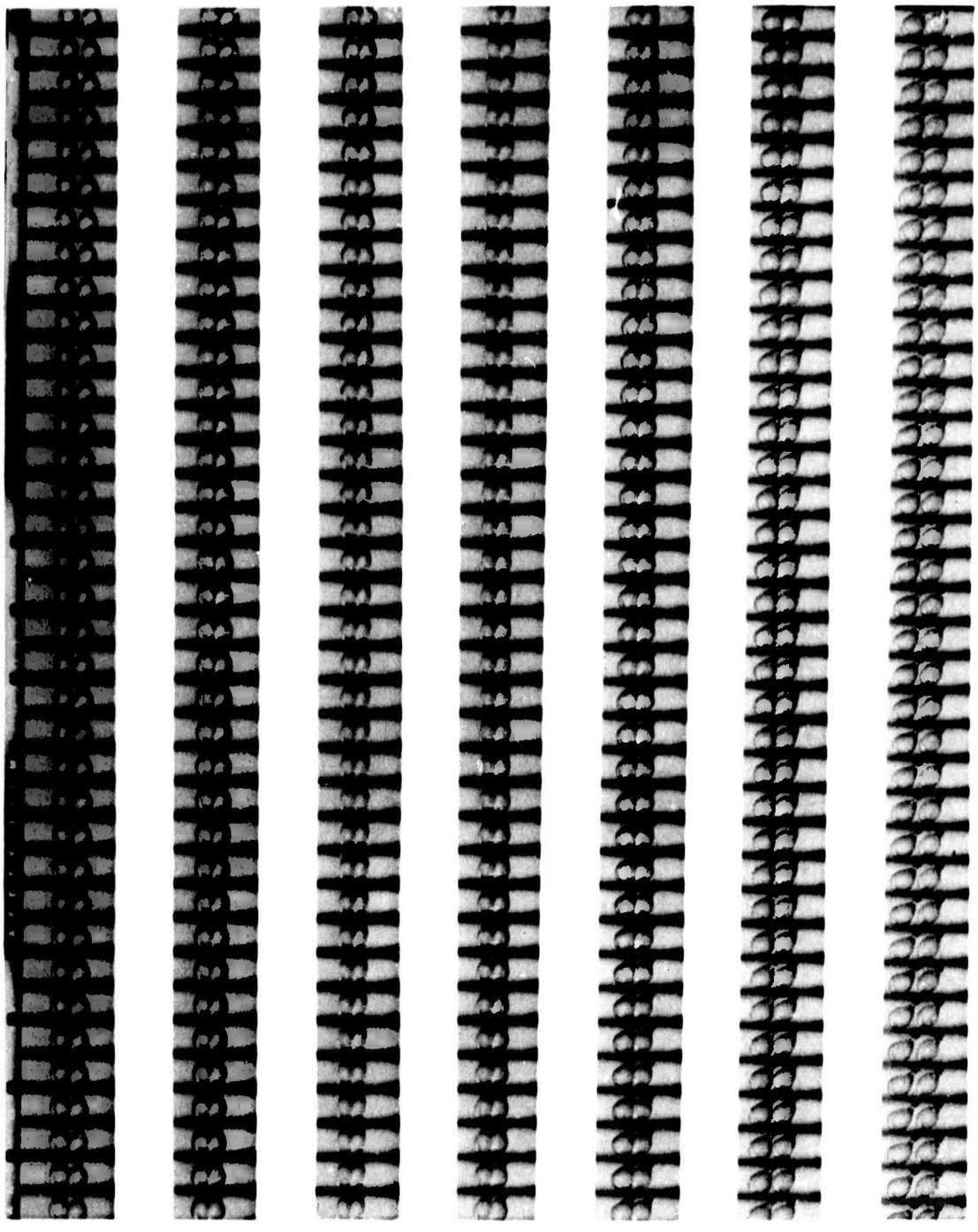

Fig. 12. A sequence of photographs taken at 14,000 frames per second of colliding and separating water drops with no potential difference.

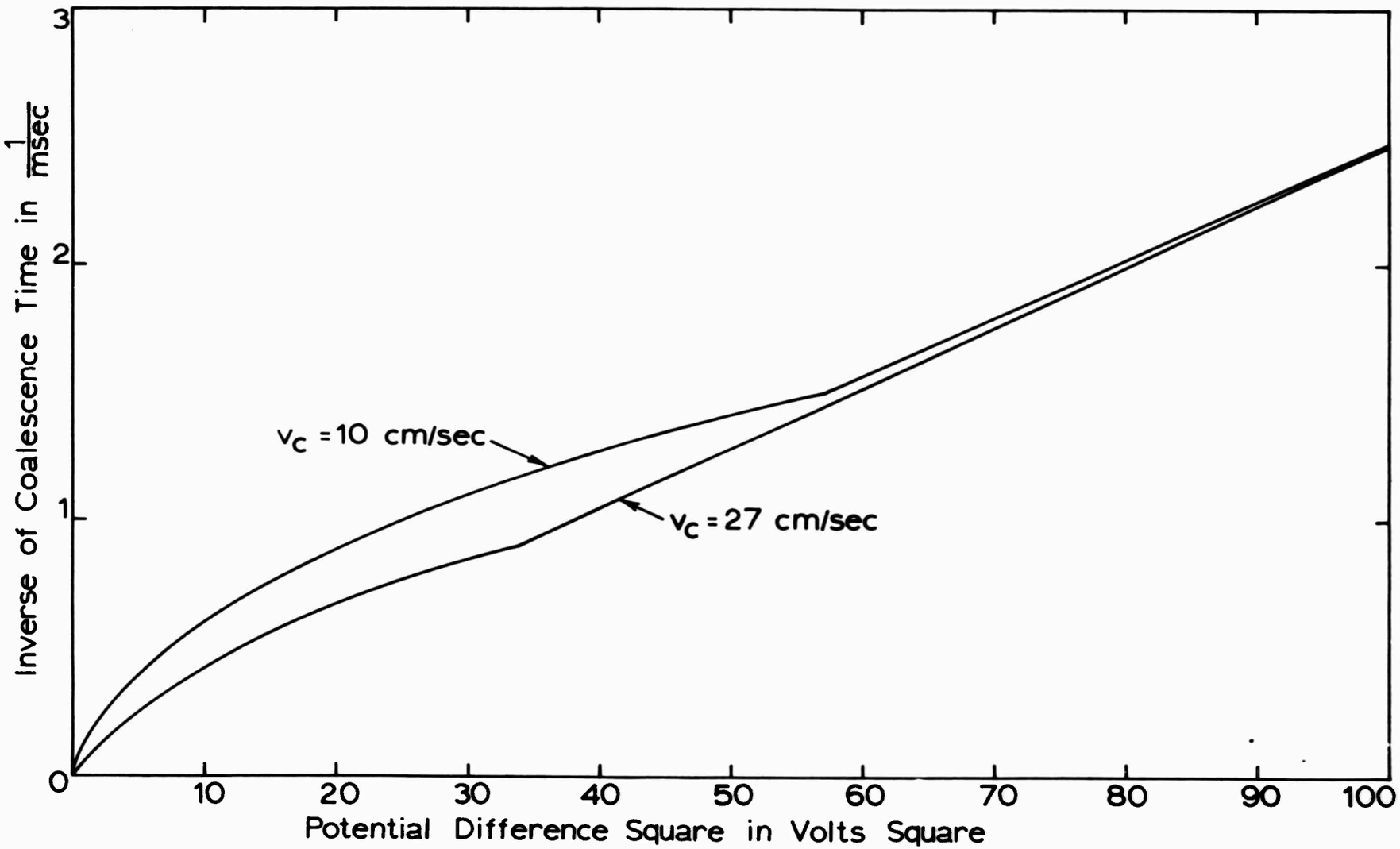

Fig. 13. A plot of the inverse of the coalescence time as a function of the square of the potential difference.

Since the making of new bonds would be proportional to the number of broken bonds, the formation of intermolecular bonds would be proportional to the V^2.

A plot of the current time is shown in Figure 14. Since the current was found to start before the apparent coalescence found on the film, this would indicate the possibility that charge was transferred between the drops before their coalescence. For very low applied voltages, the current time was very small. However, since for large applied voltages the coalescence time becomes very small, it would seem reasonable that the current time would also decrease. The maximum current time was 0.48 msec. for an applied voltage of 1.4 volts as shown in Figure 14.

The rate at which the deformation of the colliding surfaces develops is given by a plot of the height of the flattened area as a function of time as shown in Figure 15. It is observed that a single curve is common to all of the different applied voltages until the lens is formed at the time of coalescence. The growth of the lens height is more rapid than the rate of increase of the height of the flattend area. Also, the growth rate of the lens height is greater for smaller voltages than for larger voltages. The rate of growth of the lens width increased in a linear manner as shown in Figure 16, and this growth rate also proved to be less for larger voltages than for the smaller ones.

No apparent deformation of the drops was observed as the drops approached each other, but the amount of flattening of the two surfaces become much larger for the low voltages.

2.4 Discussion

The results in Figure 11 for the coalescence time shows that, as the potential between two colliding drops is increased, the amount of time the

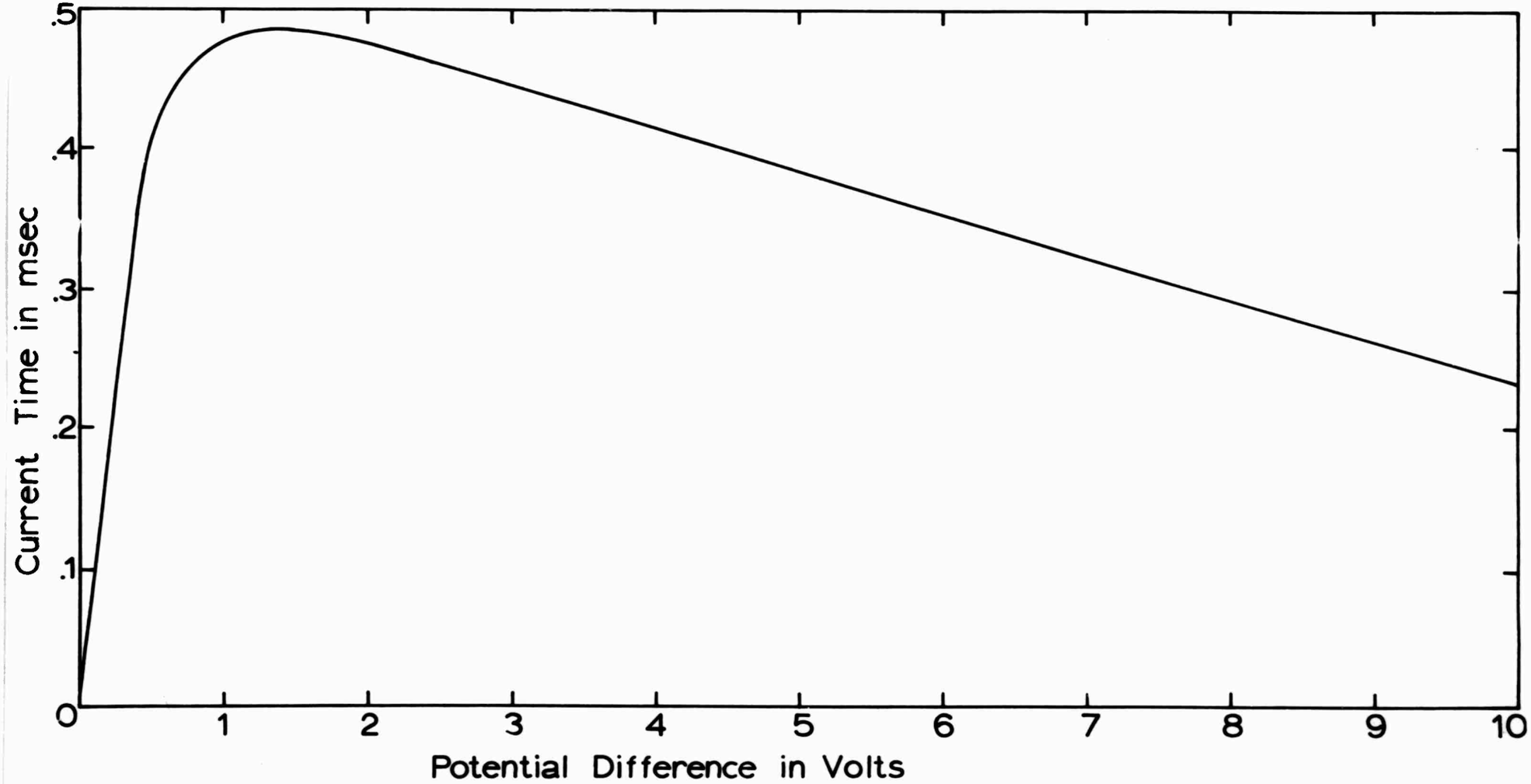

Fig. 14. A plot of the current time as a function of the potential difference between drops.

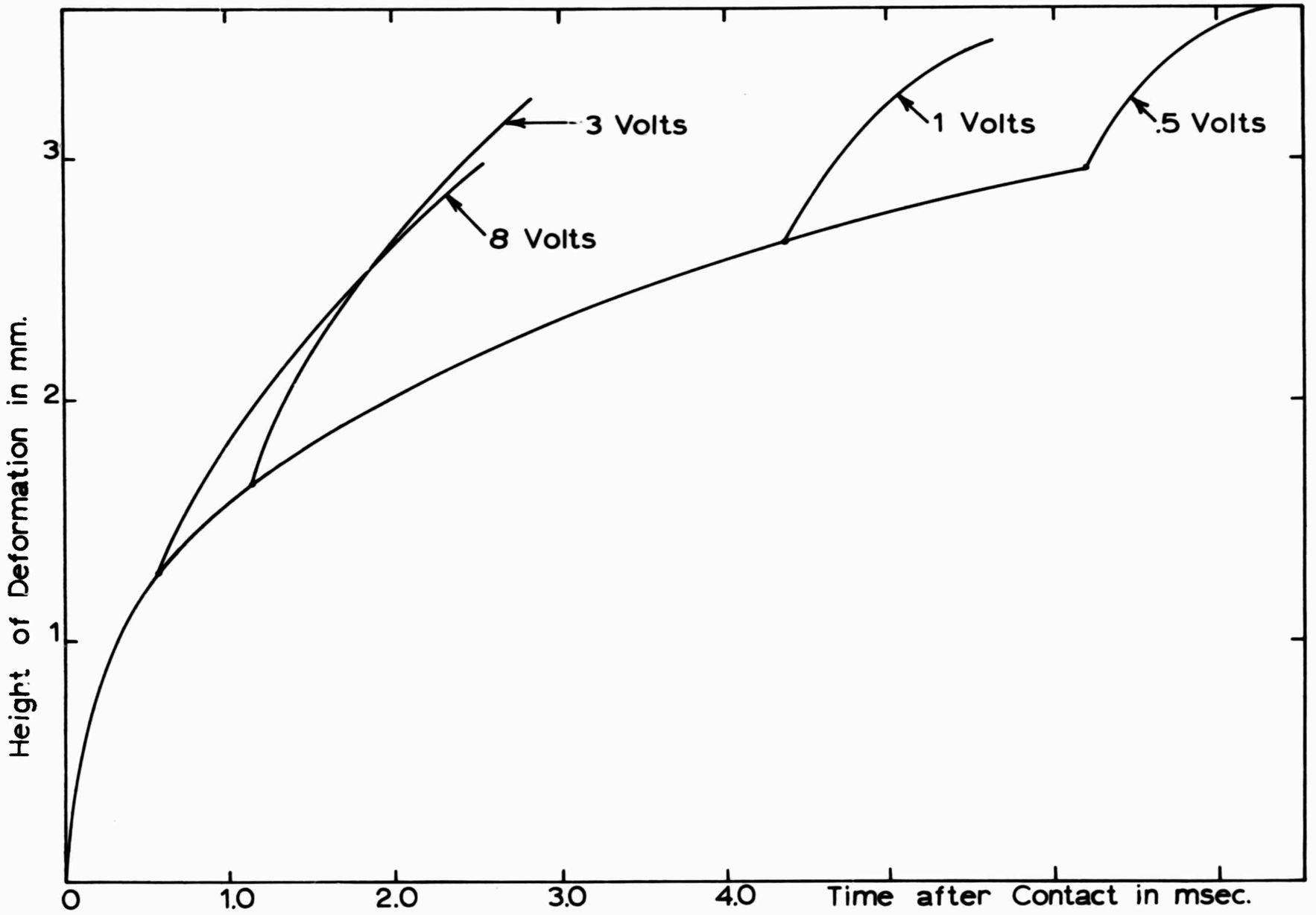

Fig. 15. A plot of the height of the flattened surface of the collided drops as a function of time after contact.

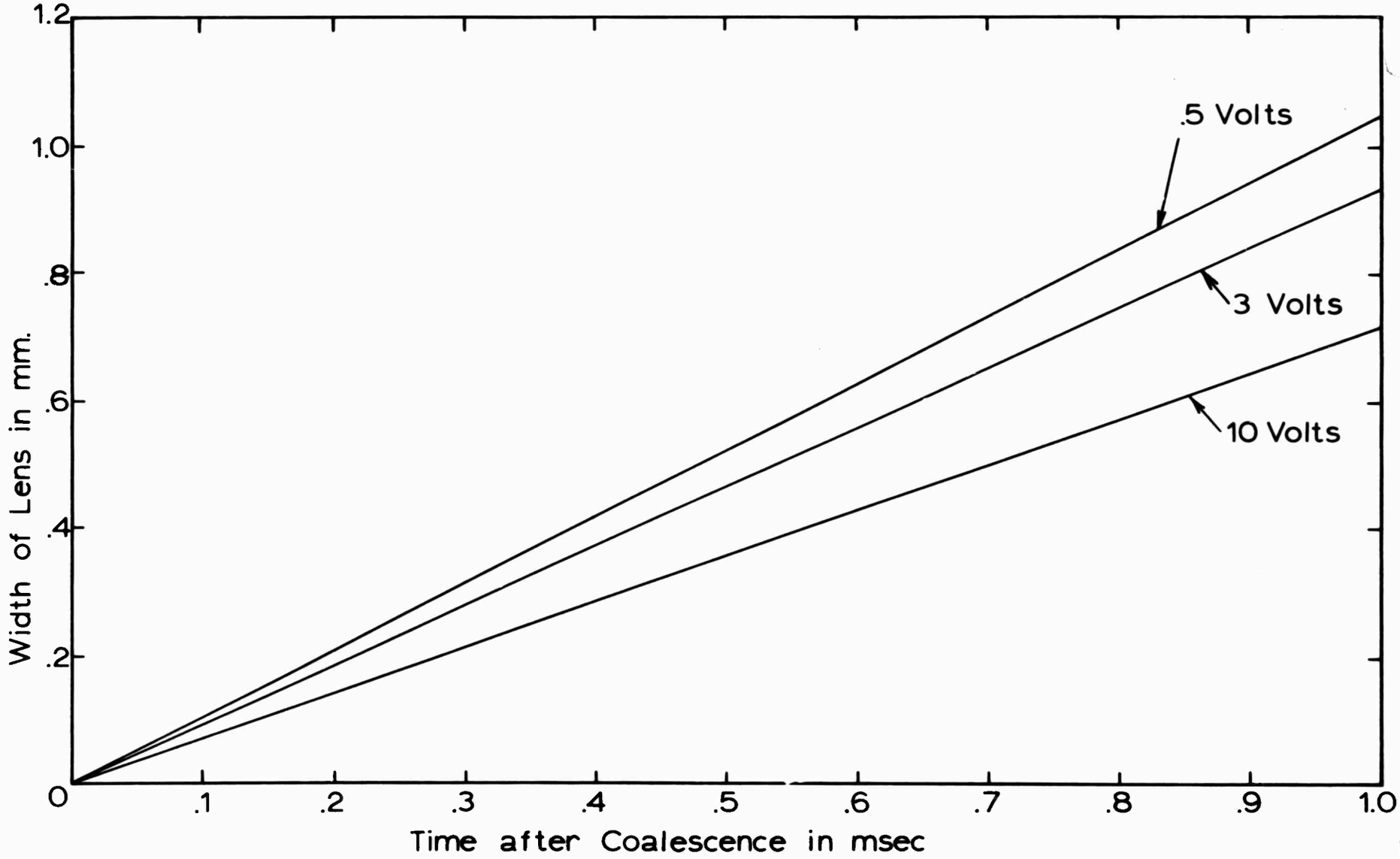

Fig. 16. A plot of the lens width as a function of time after coalescence.

two surfaces must be in contact before coalescence decreases. In nature this potential difference can be caused by either a net charge on the two drops or the presence of an external electric field. But regardless of the cause of this potential difference, the results will be the same.

The fact that the coalescence times are different for the two collision velocities at low voltages but approach each other at higher voltages, implies that for larger voltages the collision velocity becomes a secondary influence on the coalescence time. A wider range of collision velocities needs to be investigated before a final evaluation can be made.

The possibility of a charge transfer between two drops with a potential difference, as might be implied by Figure 14, is of great interest. However, no case has been observed so far during this investigation where a charge flowed between the two drops without the drops coalescing. That is, no single drop has gained a net charge by colliding with a second drop without coalescence occurring afterward. In the cases where bounce-off of the two drops was observed, no charge transfer was recorded.

It seemed reasonable that such a transfer of charge would be the result of air ionization and charge flow through this region. This would result in generating an electromagnetic wave which would be radiated from the colliding drops. In an attempt to observe this radiation a superheterodyne National Radio Receiver, NC-125, was employed. A loop antenna was placed inside the shield chamber oriented to receive the maximum radiation. To check the system, mercury drops were first used and a very strong radiation was recorded even for small applied voltages. Then water drops were used, but no radiation was observed in the range of 1-30 megacycles even for large applied voltages. No

definite conclusion can be drawn since either the radiation was too small to measure with this equipment or no radiation was transmitted. A more conclusive experiment is being sought.

BLANK PAGE

CHAPTER III

CLOUD DROPLET COLLISION EFFICIENCY IN ELECTRIC FIELDS

3.1 Introduction

The collision efficiencies reported by Lindblad and Semonin (1963a) have been extended to include the complete multipole forces between two conducting spheres as developed by Davis (1962). Lindblad and Semonin (1963a) used a simple electrostatic dipole approximation to estimate the electrical force between two spheres. These calculations show that the collision efficiency is definitely increased for cloud droplets falling in an electric field. The collision efficiency in field-free space of a 5μ droplet and a 30μ drop was calculated to be 0.02, and in a horizontal field of 3600 volts per centimeter the collision efficiency for the same pair was 0.48. This shows an increase of 2400 percent.

When the same hydrodynamics employed by Lindblad and Semonin and a slightly different form of the electrostatic force derived by Davis are used, the collision efficiency for the 30μ and 5μ pair is 0.854 in a horizontal field of 3600 volts per centimeter. This shows an increase in collision efficiency by a factor of 43 or 4,300 percent.

However, in both cases the collision efficiency in an electric field is less than unity. Contrary to these calculations Moore and Vonnegut (1959) estimate that collection efficiencies of 2.0 to 5.0 are necessary to explain the rapid appearance of rain from nonfreezing warm clouds.

3.2 Hydrodynamics

The hydrodynamics involved in the motion of two spheres was simplified by assuming the fluid containing the droplet flows around the stationary drop. This approximation ignores the mutual interactions of the flow about both spheres. The inadequacy of the above approximation is well known and has been discussed

previously by Lindblad and Semonin (1963b). The smaller drop and larger drop are defined as the 'droplet' and 'drop' respectively. The linear collision efficiencies calculated by using the stream function given by equation (1), below, as derived by Proudman and Pearson (1957), are compared in Figure 17 with the results of Hocking (1959), Pearcey and Hill (1956), and Shafrir and Neiburger (1963).

Shafrir and Neiburger approximated the mutual interactions of the flow about both spheres by solving various two-body problems. The linear collision efficiency curve for the 30μ drop lies between the curves of Shafrir and Hocking up to drop ratios of 0.42. The drop ratio is a_1/a_2 where a_1 and a_2 are the radii of the droplet and drop respectively. The linear collision efficiencies for the 40μ drop are slightly higher than Shafrir's. The linear collision efficiency curves for the 60μ drop illustrate the discrepancy between Shafrir's results and those calculated using the Proudman and Pearson stream function for larger drops. The comparison shown in Figure 17 indicates that the Proudman stream function is a good approximation for determining collision efficiencies for drops with radii less than 50μ .

The Proudman and Pearson (1957) analytical expression for the flow around the drop has the following form:

$$\Psi = \frac{1}{4}(r-1)^2(1-\cos^2\theta)\left[(1+\frac{3R}{16})(2+\frac{1}{r}) - \frac{3R}{16}(2+\frac{1}{r}+\frac{1}{r^2})\cos\theta\right] \qquad (1)$$

where the Reynolds number $R = 2\rho a_2 U/\mu$, U is the velocity of the undisturbed stream, ρ is the density, r is the radius vector between the center of the drops, θ is the angle between r and the x axis measured positively in the clockwise direction, and μ is the dynamic viscosity of air. The geometry is shown in Figure 18.

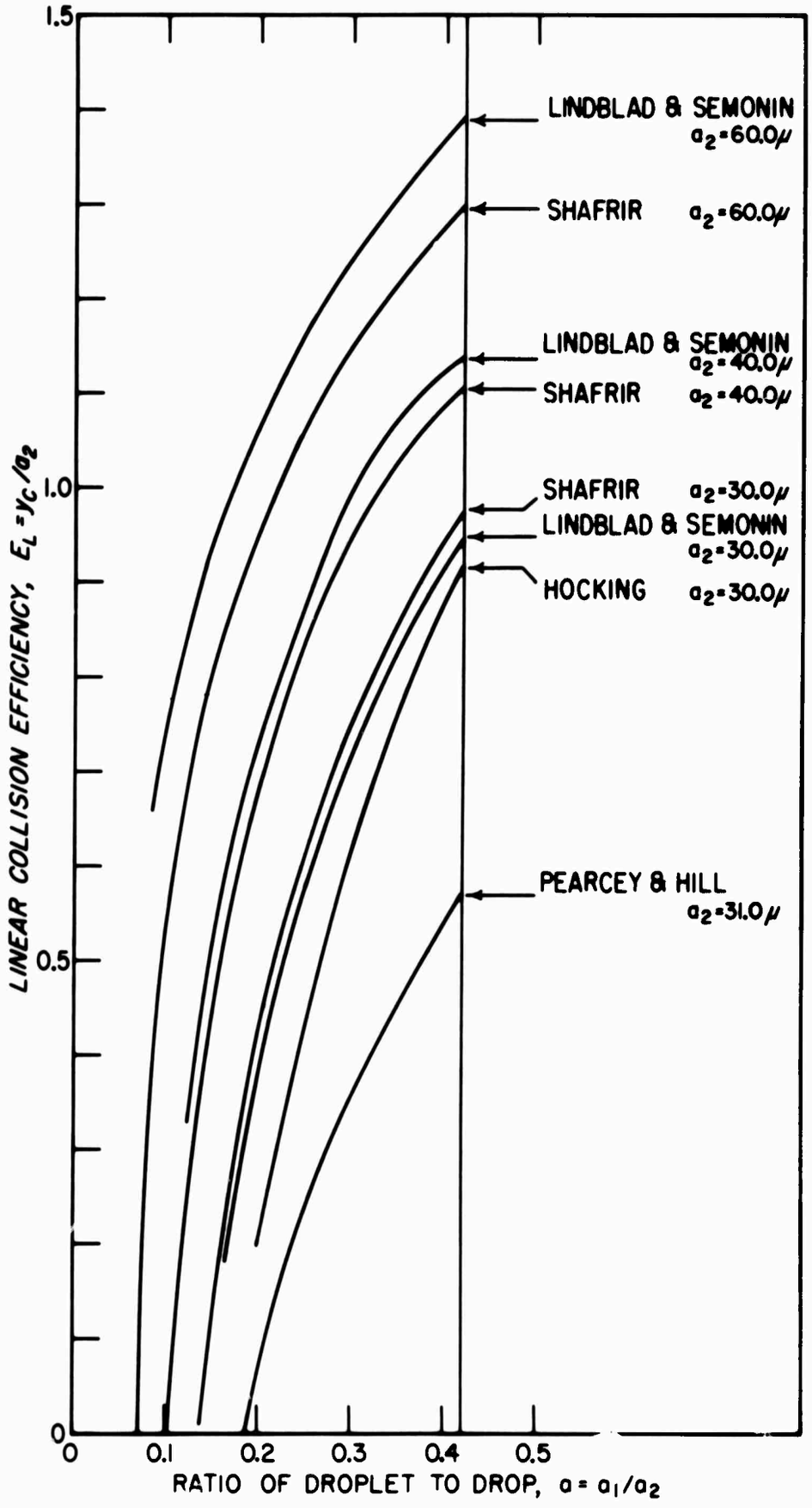

Fig. 17 Comparison of linear collision efficiency as calculated by various authors.

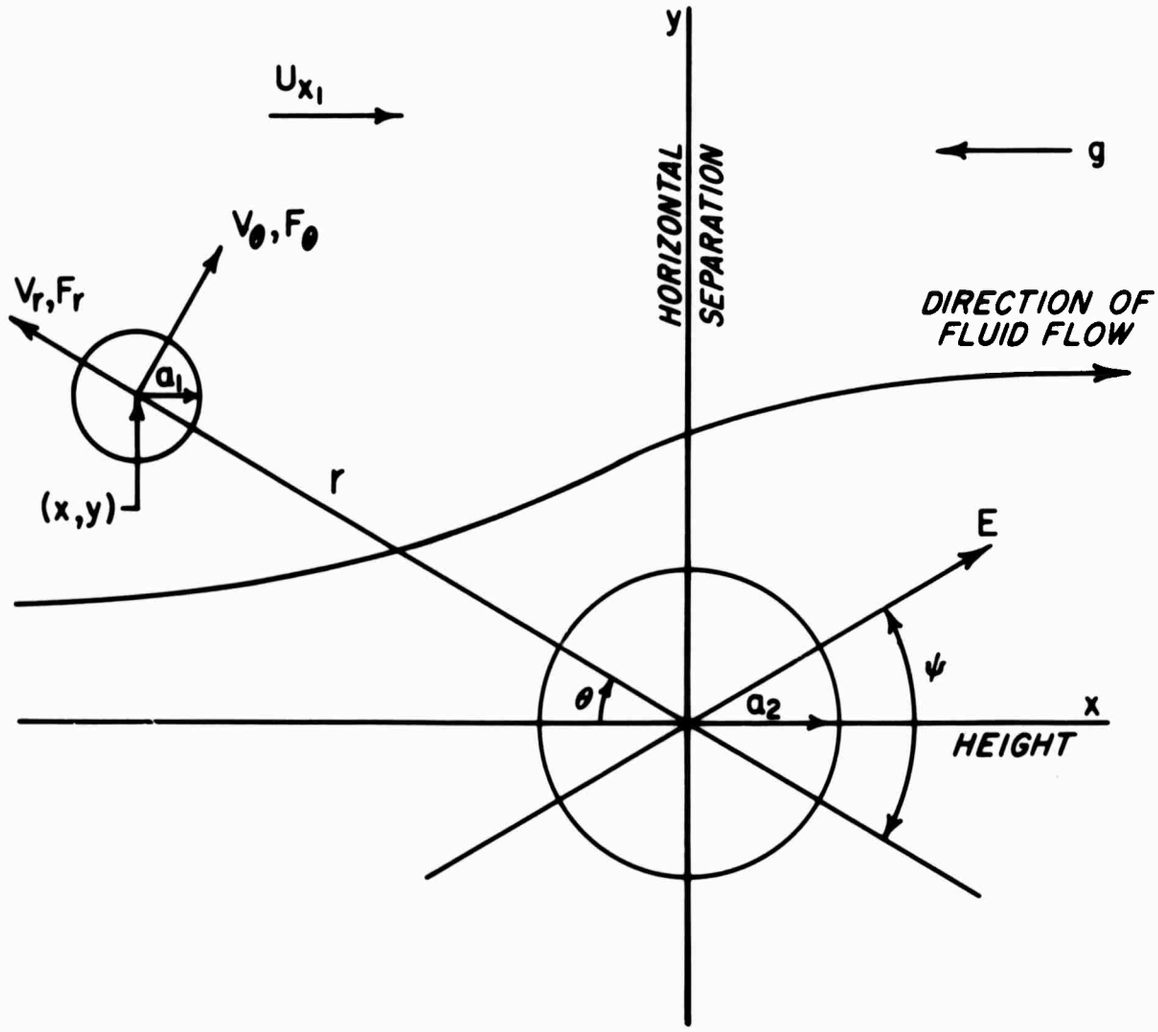

Fig. 18 Motion of a droplet in an electric field, E, relative to a fixed drop.

3.3 Electrostatics

A specific problem of two conducting rigid spheres in a uniform electric field has been solved by Davis (1962). One justification for using these solutions to approximate two water drops can be shown by the use of the continuity equation for charge. It follows that charge density within a drop is given by the equation $\partial\rho'/\partial t + \sigma'\rho'/\epsilon = 0$ where ϵ is the permittivity of water, σ' is the conductivity of water, and ρ' is the charge density. Therefore the charge density is proportional to $e^{-\sigma' t/\epsilon}$, and the time constant ϵ/σ', called the relaxation time, for water is 10^{-6} sec. Thus the electric field intensity within the drop decreases rapidly to zero with time, justifying the assumption that water is a good conductor.

Water droplets, with radii considered in this report, are distorted only a small amount when falling at their terminal velocities. This distortion and the deformation which occurs because of electrical forces when the droplets are close are neglected.

Davis (1962) solved the problem of two conducting rigid spheres by first determining the surface charge density, σ, on the conducting spheres in a uniform electric field. The net force in the MKS system of units on each sphere was computed by integrating the surface stress $\sigma^2/2\epsilon_o$ over each sphere, where ϵ_o is the permittivity of free space. The force on the droplet was given as follows:

$$F_r = F'_r + q_1 E\cos\psi \qquad (2)$$

$$F_\theta = F'_\theta + q_1 E\sin\psi \qquad (3)$$

where

$$F'_r = 4\pi\epsilon_o\alpha^2 \sum_{N=0}^{\infty} A_N e^{(2N+1)\mu_1}\left[A_N(2n+1) - A_{n+1}(n+1)(e^{2\mu_1+1})\right]$$

$$+ 8\pi\epsilon_o\alpha^2\, E^2\sin^2\psi \sum_{n=0}^{\infty} B_n\, n(n+1)e^{(2n+1)\mu_1}\left[B_n(2n+1) - B_{n+1}(n+2)(e^{2\mu_1+1})\right]$$

$$F'_\theta = 4\pi\epsilon_o\alpha^2\, E\sin\psi\,(e^{2\mu_2}-1) \sum_{n=0} (n+1)e^{(2n+1)\mu_1}\left[A_{n+1}B_n n - A_n B_n(n+2)\right]$$

The coefficiencies are given as:

$$A_n = \frac{E\cos\psi\,(2n+1)(e^{(2n+1)\mu_{2+1}}) - (\frac{1/2}{\alpha})e^{(2n+1)\mu_2} + (\frac{V_1}{\alpha})}{e^{(2n+1)\mu_o} - 1}$$

$$B_n = \frac{e^{(2n+1)\mu_2} - 1}{e^{(2n+1)\mu_o} - 1}$$

where

$$V_1 = P_{11}(q_1 - Q_1) + P_{12}(q_2 - Q_2) \qquad (4)$$

$$V_2 = P_{12}(q_1 - Q_1) + P_{22}(q_2 - Q_2) \qquad (5)$$

and

$$Q_1 = -8\pi\epsilon_o\alpha^2\, E\cos\psi \sum_{n=0}^{\infty} (2n+1)\,\frac{e^{(2n+1)\mu_{2+1}}}{e^{(2n+1)\mu_{o-1}}}$$

$$Q_2 = 8\pi\epsilon_o\alpha^2\, E\cos\psi \sum_{n=0}^{\infty} (2n+1)\,\frac{e^{(2n+1)\mu_{1+1}}}{e^{(2n+1)\mu_{o-1}}}$$

$$P_{11} = \frac{C_{22}}{C_{11}C_{22} - C^2_{12}}$$

$$P_{22} = \frac{C_{11}}{C_{11}C_{22} - C_{12}^2}$$

$$P_{12} \quad \frac{-C_{12}}{C_{11}C_{22} - C^2_{12}}$$

The capacities of the two spheres are given as:

$$C_{11} = 8\pi\epsilon_o\alpha \sum_{n=0}^{\infty} \frac{e^{(2n+1)\ 2}}{e^{(2n+1)\ o}-1}$$

$$C_{12} = -8\pi\epsilon_o\alpha \sum_{n=0}^{\infty} \frac{1}{e^{(2n+1)\ o}-1}$$

$$C_{22} = 8\pi\ _o\alpha \sum_{n=0}^{\infty} \frac{e^{(2n+1)\ 1}}{e^{(2n+1)\ o}-1}$$

where

$$e^{\mu_1} = \frac{C_1 + \alpha}{a_1} \quad , \quad e^{\mu_2} = \frac{C_2 + \alpha}{a_2} \quad , \quad e^{\mu_o} = e^{(\mu_1 + \mu_2)}$$

$$\alpha = (C^2_1 - a^2_1)^{1/2}$$

$$C_1 = (r^2 + a^2_1 - a^2_2)/2r$$

$$C_2 = (r^2 + a^2_2 - a^2_1)/2r$$

In the above equations E is the applied electric field, ψ is the angle between the electric field and the line joining the centers as illustrated in Figure 18, and q_1 and q_2 are the net charges on the droplet and drop respectively. For uncharged droplets falling in an external electric field q_1 and q_2 are zero.

3.4 Equations of Motion

The equations of motion for the droplet subjected to electrical forces are

$$M_1 dU_{x1}/dt = -6\pi\mu a_1(U_{x1} - U_x)Cd_1R_1/24 - M_1 g + F_x \qquad (6)$$

$$M_1 dU_{y1}/dt = -6\pi\mu a_1(U_{y1} - U_y)Cd_1R_1/24 + F_y \qquad (7)$$

where the subscript 1 refers to the droplets, Cd_1 is the drag coefficient, U_x and U_y are the x and y components of the stream velocity, and F_x and F_y are the electrical forces. The stream velocities were determined from

$$U_x = - V_r \, Cos\theta + V_\theta \, Sin\theta \qquad (8)$$

$$U_y = V_r \, Sin\theta + V_\theta \, Cos\theta \qquad (9)$$

where

$$V_r = - \frac{1}{r^2 \, Sin\theta} \frac{\partial \Psi}{\partial \theta} \quad \text{and} \quad V_\theta = \frac{1}{r \, Sin\theta} \frac{\partial \Psi}{\partial r}$$

To obtain F_x and F_y the following transformation was used

$$F_x = - F_r \, Cos\theta + F_\theta \, Sin\,\theta$$

$$F_y = F_r \, Sin\theta + F_\theta \, Cos\,\theta$$

where F_r and F_θ are given by (2) and (3).

The equations of motion were made dimensionless before integration on the IBM 7094 computer. The unit of length was a_2, which is the radius of the drop, and the unit of velocity was U, which is the velocity of the undisturbed stream at infinity.

3.5 Initial Conditions

To compare these results with those previously reported by Lindblad and Semonin the same initial conditions were used. The results of Gunn and Kinzer (1949) were used to determine the terminal velocity, drag coefficient, and Reynolds number for distilled water drops in stagnant air at 760 mm pressure, 50 percent relative humidity, and 20°C.

The initial vertical separation was 50 drop diameters, and the initial horizontal separation was one drop diameter. The grazing trajectory was called y_c, and the collision efficiency was defined as

$$E_c = y_c^2/(a_1 + a_2)^2 \qquad (10)$$

Eight trajectories were used to calculate the collision efficiency. The horizontal separation for the first trajectory was always $y_1 = a_2$. If the first trajectory resulted in a hit, then the next horizontal separation selected by the computer was $y_2 = y_1 + 1/2$, or in case of a miss $y_2 = y_1 - 1/2$. In general, we have $y_{k+1} = y_k \pm (1/2)^k$ where $k \leq 7$. The grazing trajectory was defined as $y_c = 1/2\ (y_{hit} + y_{miss})$, where y_{hit} and y_{miss} are the last hit and miss.

3.6 Conclusions

The effects of both horizontal and vertical electric fields on the collision efficiency are shown in Figures 19, 20, and 21. The trajectories for the 30 μ drop and 5 μ droplet, and the 40 μ drop and 5 μ droplet are shown in Figures 22 and 23. In all cases there was a definite increase in collision efficiency over those previously reported by Lindblad and Semonin which are depicted by the dashed curves in Figures 19, 20, and 21. For low fields (less than 1,000 volts per centimeter) where the dashed curves are essentially flat, the more sophisticated electrical force shows an increase in most cases. A few collision efficiencies were calculated at 6,000 and 10,000 volts per centimeter to see if they exceeded unity. These are shown in Figures 24 and 25. For these very large electric fields, collision efficiencies greater than one and two were calculated. Electric fields as large as 6,000 to 10,000 volts per centimeter may be unrealistic since they have not been measured in electrified clouds.

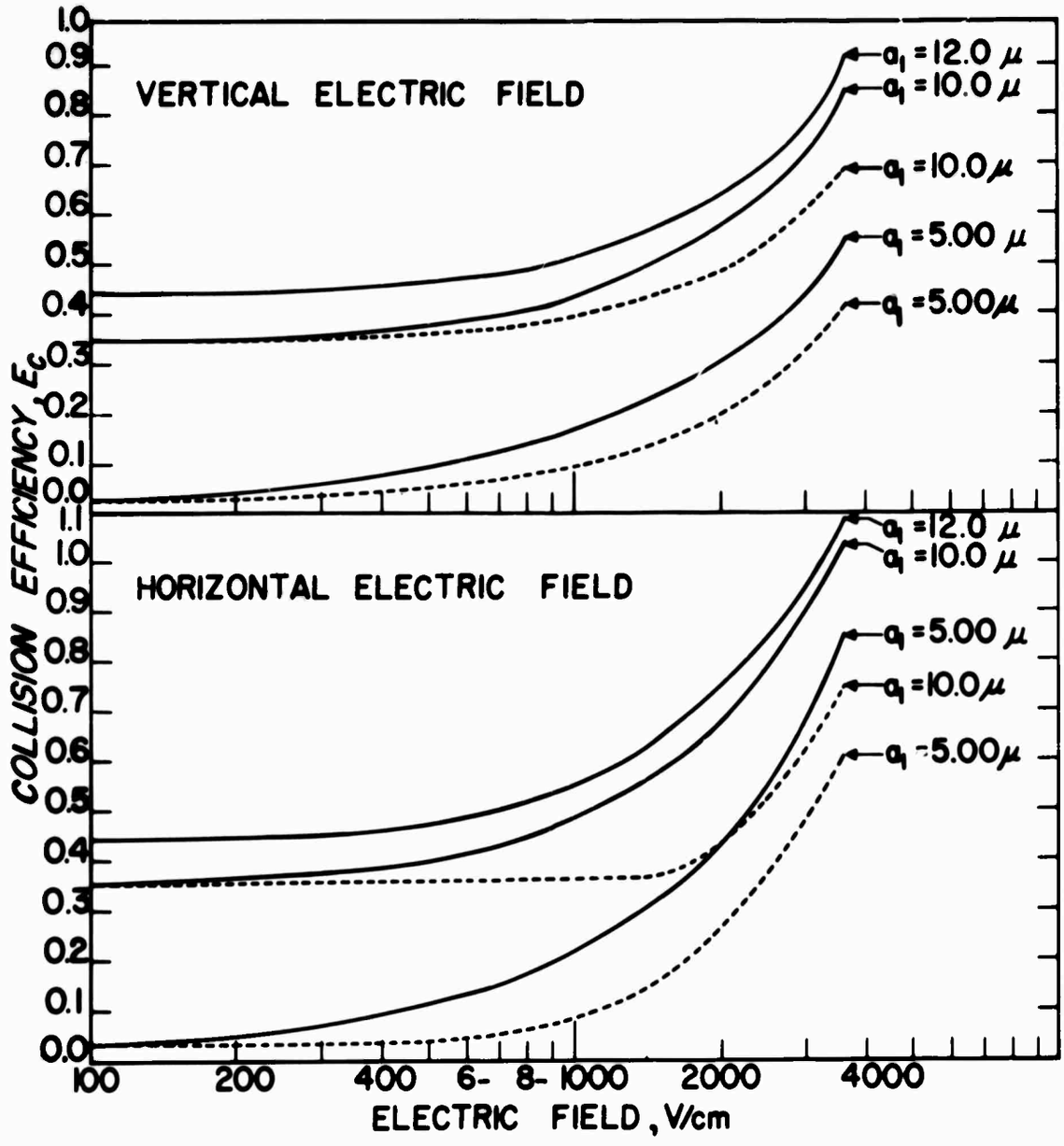

Fig. 19. Collision efficiency curves for a 30 μ drop with a 5, 10, and 12.0 μ droplet.

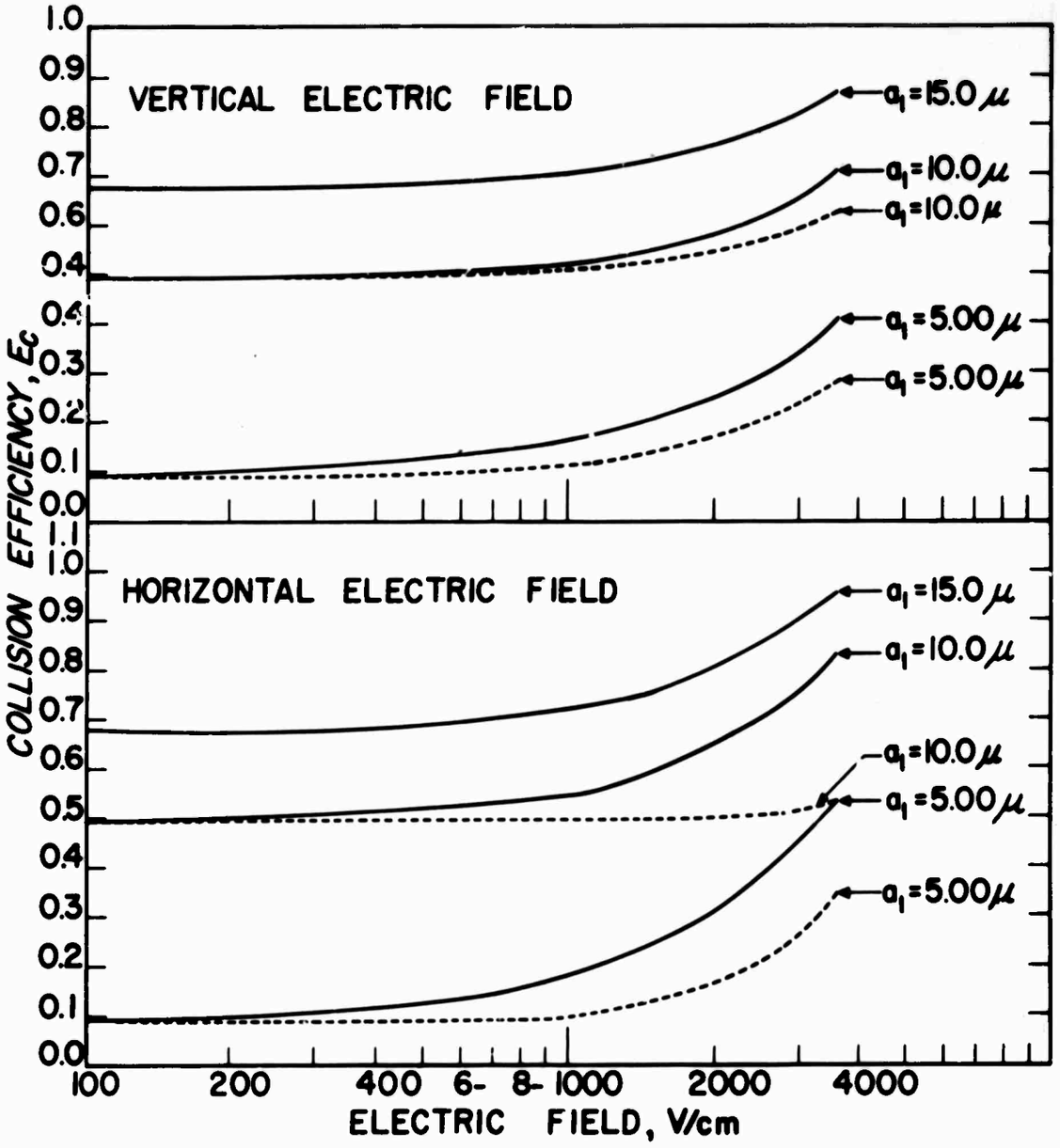

Fig. 20. Collision efficiency curves for a 40μ drop with a 5, 10, and 15μ droplet.

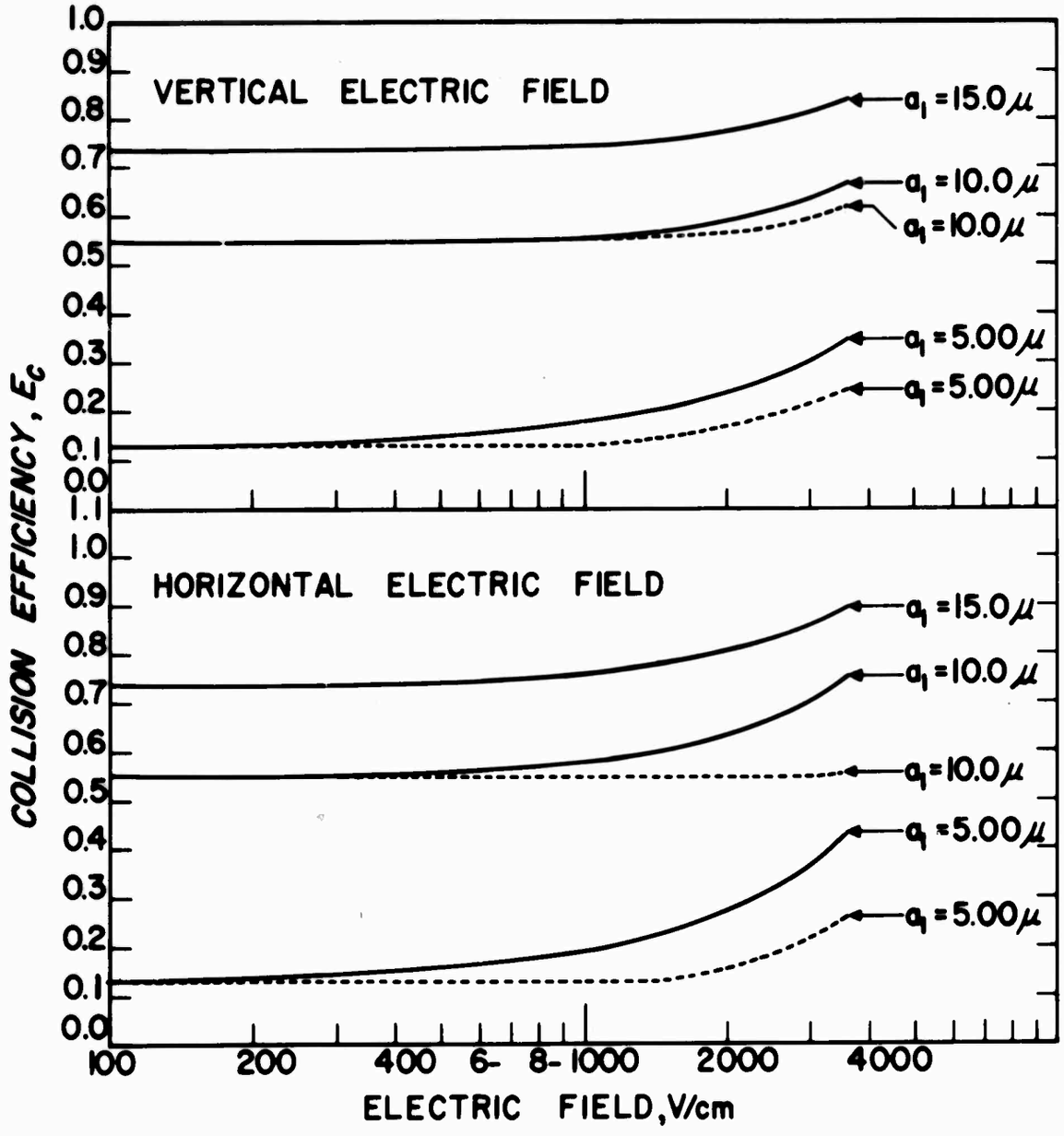

Fig. 21. Collision efficiency curves for a 50μ drop with a 5, 10, and 15μ droplet.

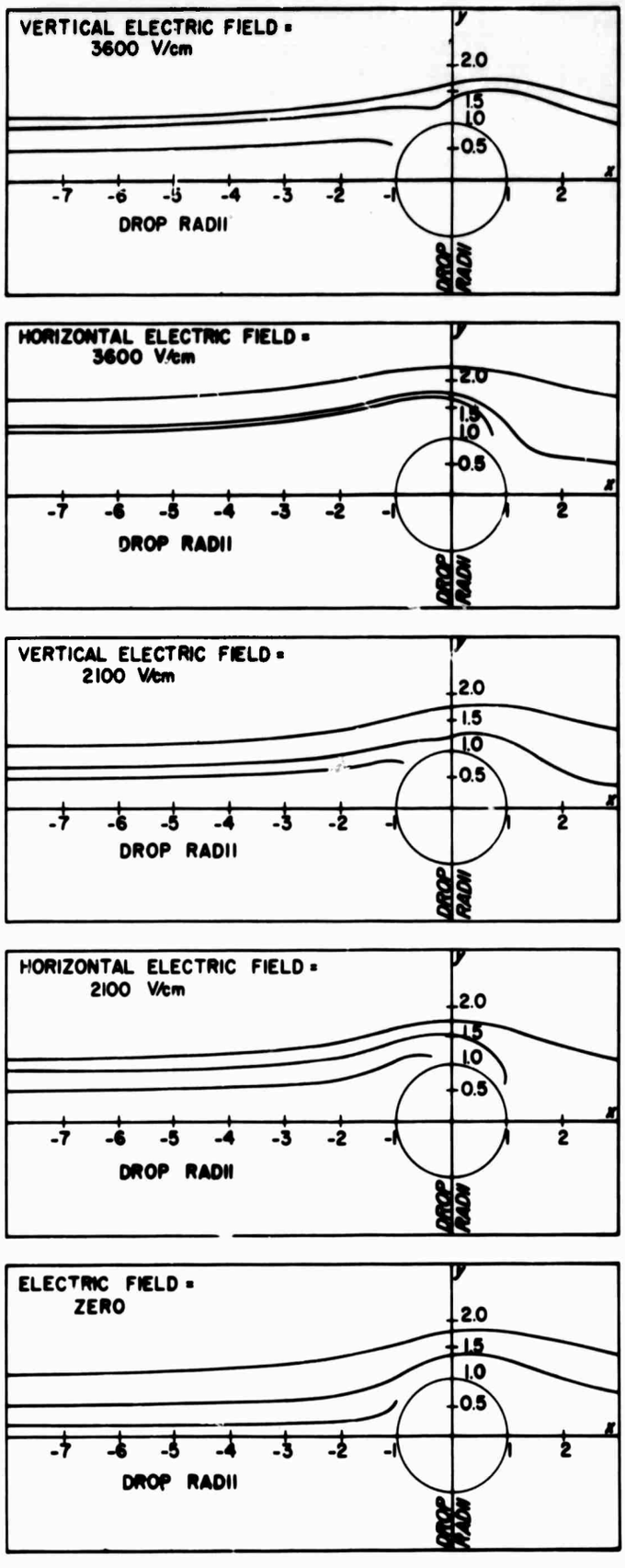

Fig. 22 Trajectories for a 30 μ drop and 5 μ droplet.

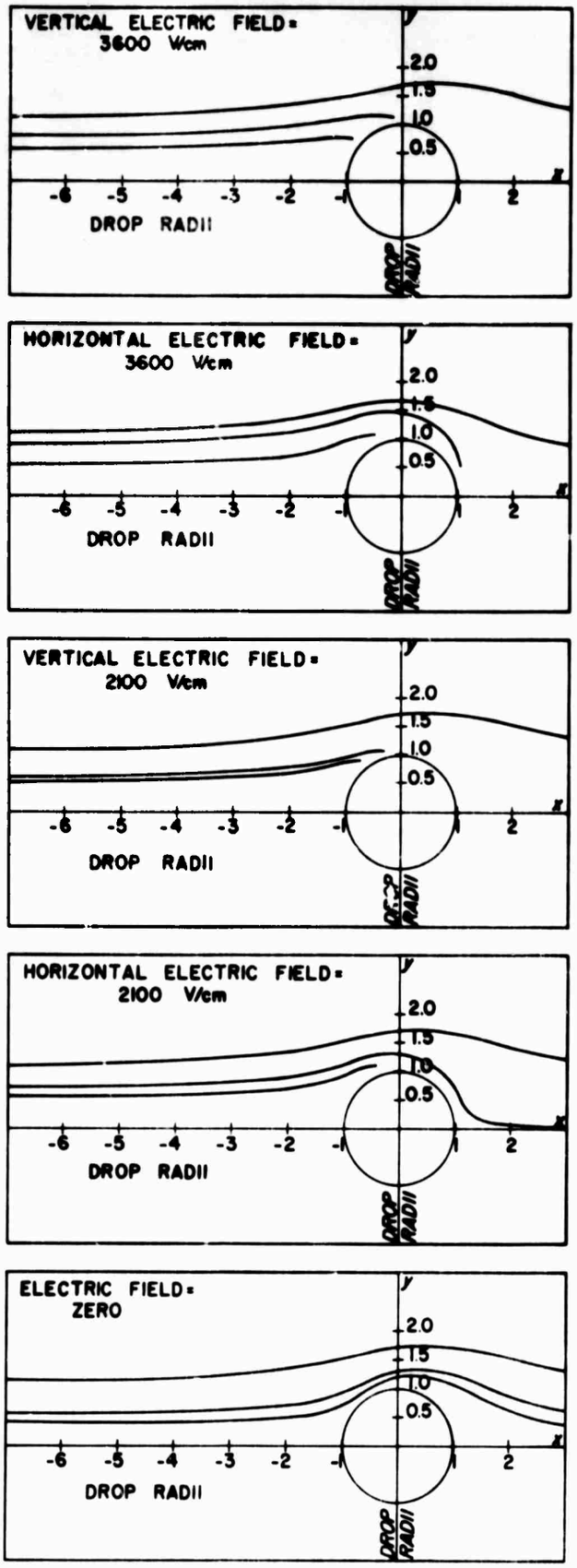

Fig. 23 Trajectories for a 40μ drop and a 5μ droplet.

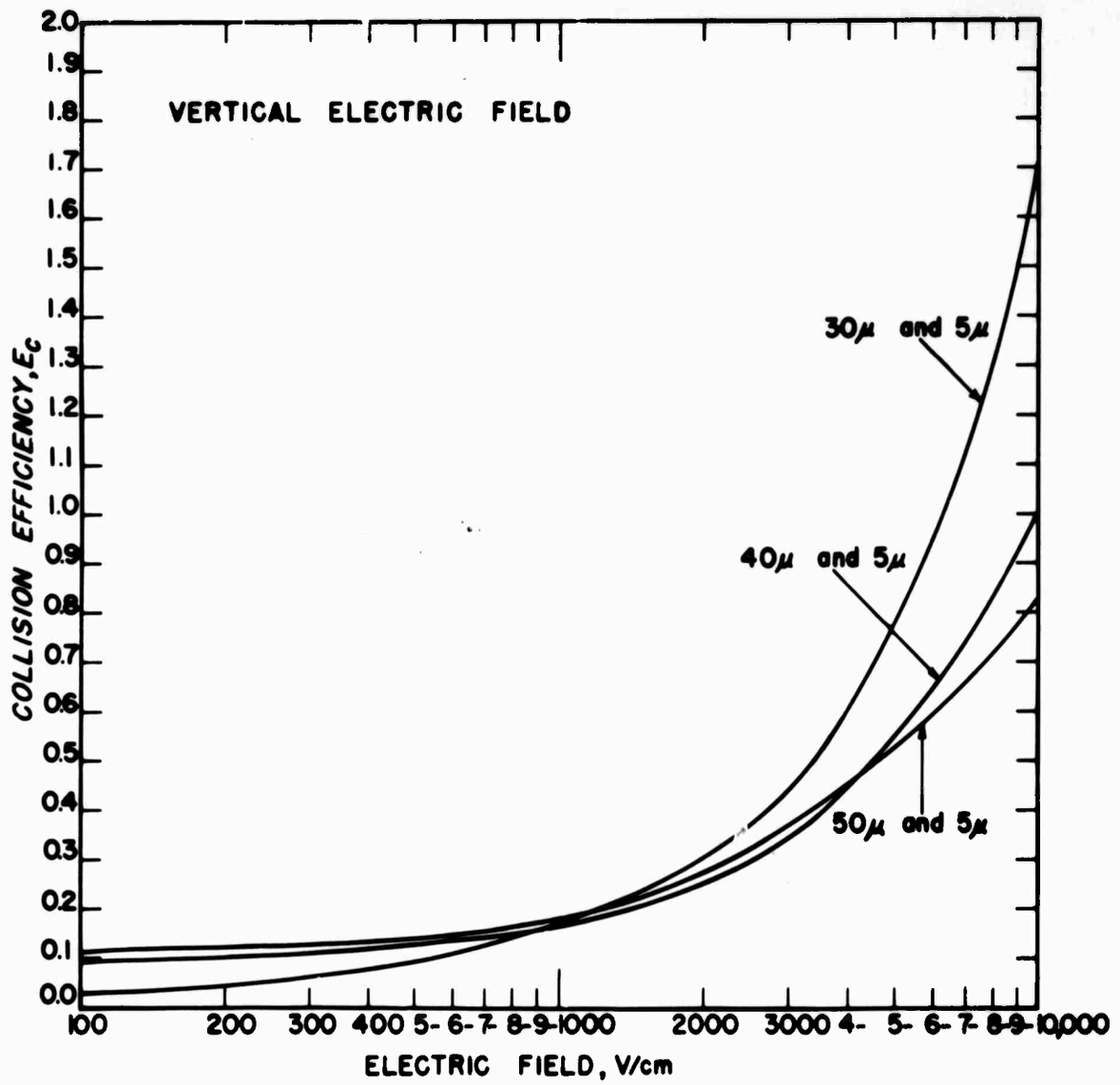

Fig. 24. Collision efficiency curves of various drop pairs in large vertical electric fields.

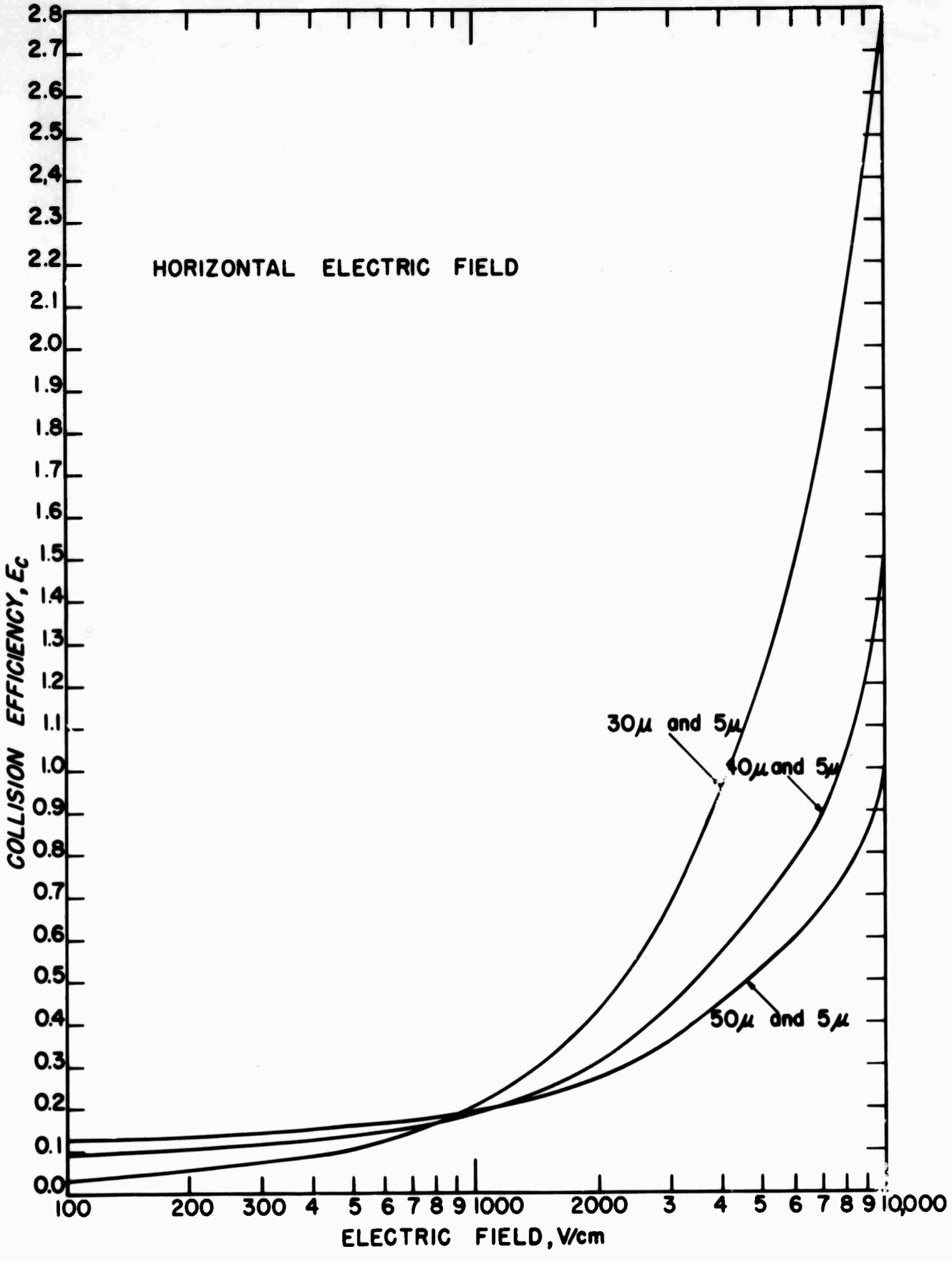

Fig. 25 Collision efficiency curves of various drop pairs in large horizontal electric fields.

The trajectories plotted in Figures 22 and 23 show that some of the droplets falling in a horizontal electric field collided with the back side of the drop, i.e., for $0 \leq x \leq 1$. In a vertical electric field this is less likely to occur because of the region of repulsion that exists (Lindblad and Semonin, 1963a). When the droplets enter the repulsion region, they are forced away from the drop, thus making the collision efficiencies lower in the vertical electric fields

For 3600 volts per centimeter at various orientations, the change in the collision efficiency for various drop pairs is shown in Figures 26 and 27, where β is the angle between the electric field, E, and the x-axis measured positively in the clockwise direction (See Figure 28).

To calculate the collision efficiency as a function of β, droplets in both half-planes ($y > 0$ and $y < 0$) had to be examined. If, for example, the electric field is oriented at an angle $\beta = 45^{\circ}$ as shown in Figure 28 then, because of the electrical forces due to the surface charge distribution, the droplet in the half-plane $y > 0$ will have a higher collision efficiency than the droplet in the half-plane $y < 0$. If y_c and y'_c are the grazing trajectories then the collision efficiency was defined as

$$E'_c = (y_c + y'_c)^2 / 4(a_1 + a_2)^2 .$$

For the four special cases $\beta = 0, \frac{\pi}{2}, \pi$, and $3\frac{\pi}{2}$ the last equation reduces to (10) because of symmetry $y_c = y'_c$. Figures 26 and 27 show that largest collision efficiencies occur approximately in the range for $50^{\circ} < \beta < 130^{\circ}$ and the lowest collision efficiency for approximately $\beta = 42^{\circ}$ and 138°. The maximum collision efficiency occurs for $\beta = \pi/2$ (i.e., a horizontal electric field).

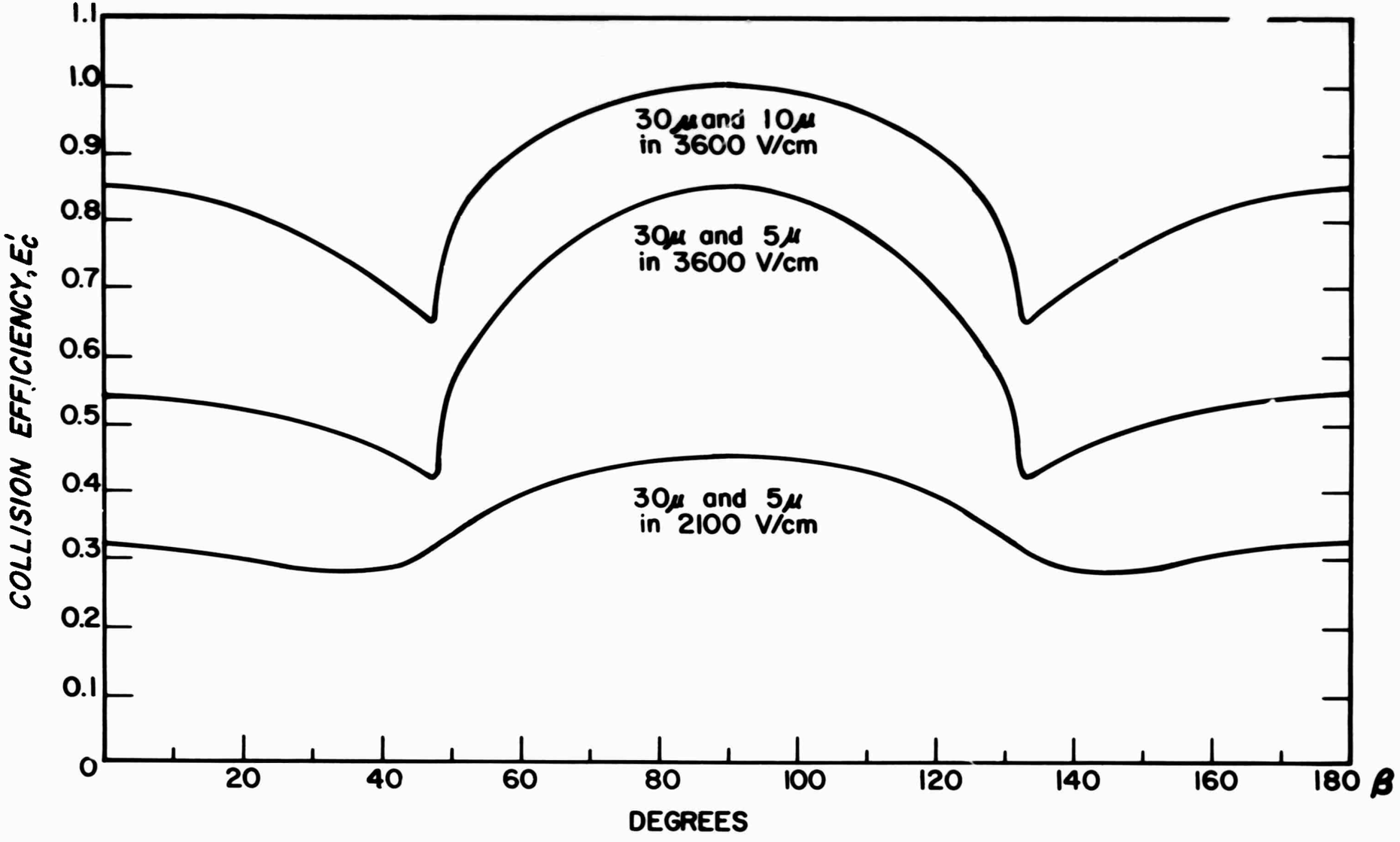

Fig. 26 Change in collision efficiency of drop pairs for various orientations of electric field.

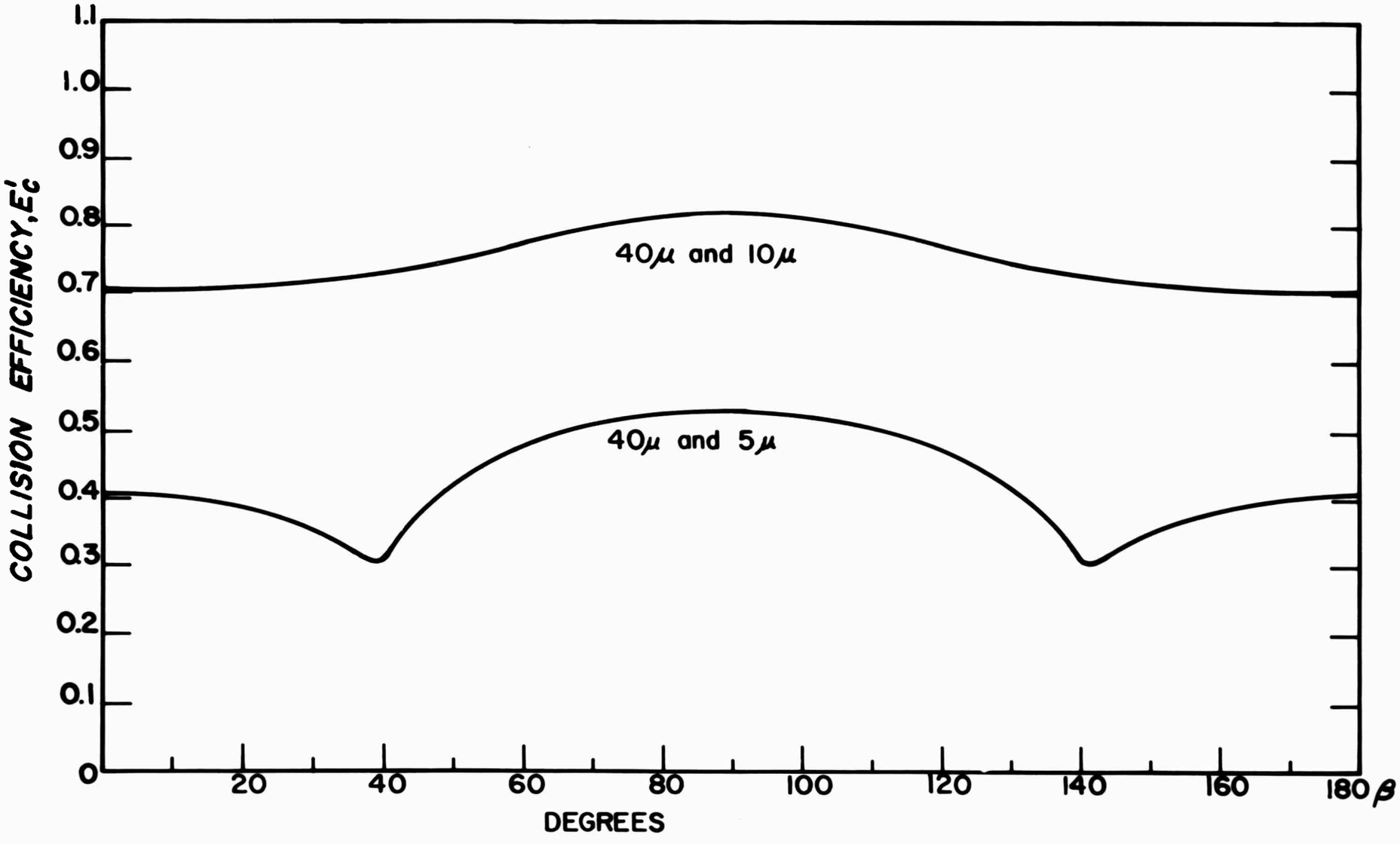

Fig. 27 Change in collision efficiency of drop pairs for various orientations of electric field at 3,600 volts per centimeter.

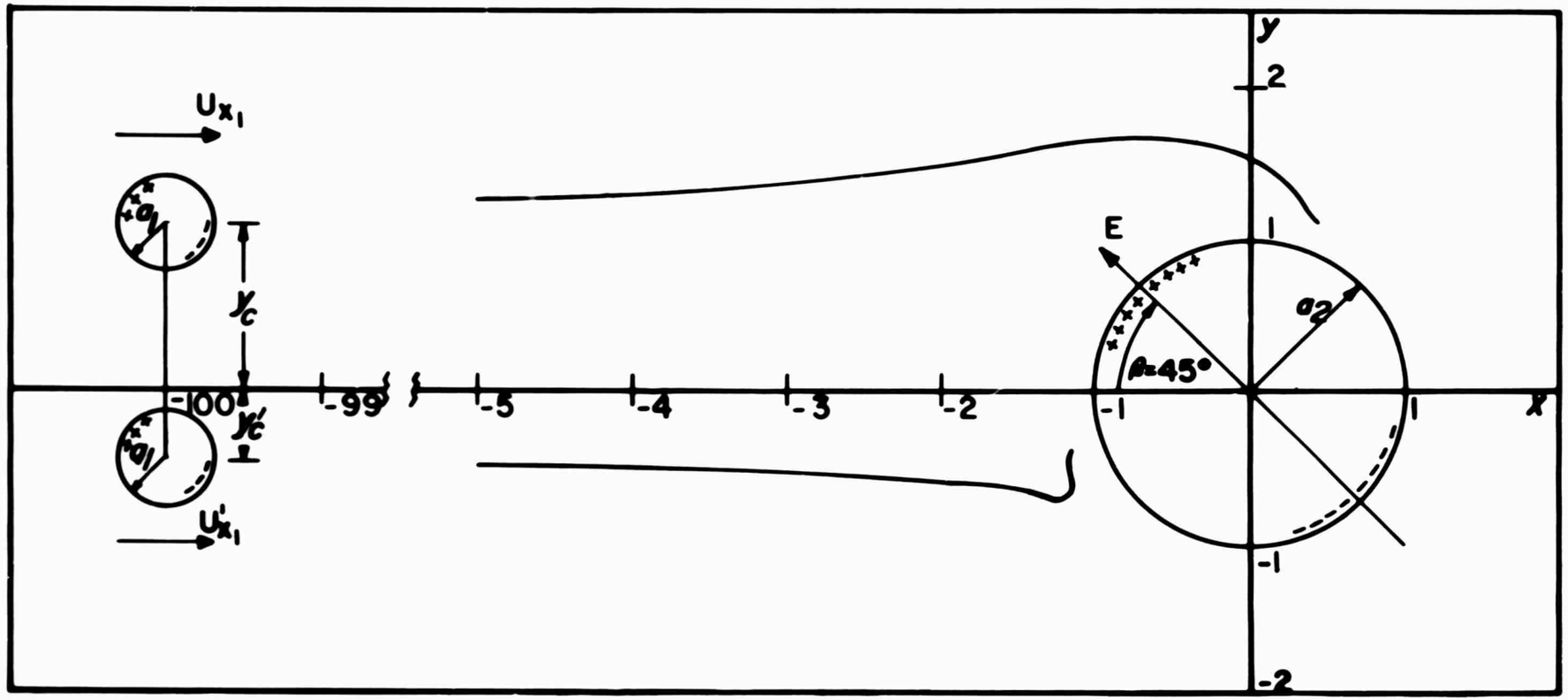

Fig. 28. The grazing trajectories in the half-plances ($y>0$ and $y<0$) for a 30μ drop and a 5μ droplet in an electric field oriented at $\beta = 45^{o}$.

The collision efficiency increases exponentially for horizontal and vertical electric fields greater than 1,000 volts per centimeter. The maximum and minimum collision efficiencies for arbitrary orientations of electric field with respect to the direction of fall occurred for $\beta = 90^{o}$, and 270^{o} and $\beta = 42^{o}$, and 138^{o} respectively.

The two-body problem is presently in the programming stage. The Shafrir and Neiburger (1963) hydrodynamic solution for two bodies will be used to approximate the mutual interaction of the flows, and the Davis (1962) electrostatic solution of the force between two spheres will be used to calculate the electrical force between drop and droplet. With Shafrir's solution one can examine drops of nearly equal size. For large drop ratios the relative velocity will be small, and one would expect large increases in collision efficiencies for drops falling in electric fields.

BIBLIOGRAPHY

1. Allan, R. S., Charles, G. E., and Mason, S. G.,(1961), J. Colloid Sci. 16, 150.

2. Berg, T. G. Owe, Fermish, G. C., and Gaukler, T. A., (1963), J. Atmos. Sci. 20, 153.

3. Bergeron, T., 1935: "On the physics of clouds and precipitation," Proc. 5th Assembly U.G.G.I., Lisbon, 156-178.

4. Best, A. C., 1951: "The size of cloud droplets in layer-type clouds," Quart. J. Roy. Meteorol. Soc., 77, 241-248.

5. Davis, M. H., 1962: The forces between conducting spheres in a uniform electric field, Rand Corp. Memorandum RM-2607-1PR.

6. Derjaguin, B. V., and Kussakov, M., (1939) Acta Physicochim, U.R.S.S., 10, 25.

7. Elton, G. A. H., (1948), Proc. Roy. Soc. (London) A194, 275.

8. Elton, G. A. H. and Picknett, R. G., (1957), "Proceedings of the 2nd International Congress of Surface Activity", Vol. 1, p. 287, Butterworths, London.

9. Findeisen, W., 1938: "Colloidal-meteorological processes during formation of precipitation," Met. Zeits, 55, 121-133. Translated by M. Sharenow, Met. Br., Evans Sig. Lab., Belmar, N. J.

10. Geoffrey, T. B., and LaMer, V. K., (1962), "Retardation of Evaporation by Monolcayers: Transport Processes", p. 9, Academic Press, New York.

11. Gunn, R., and G. B. Kinzer, 1949: The terminal velocity of fall for water drops in stagnant air. J. Meteorol., 6, 243-248.

12. Hocking, L. M., 1959: The collision efficiency of small drops, Quart. J. Roy. Meteorol. Soc., 85, 44-50.

13. Houghton, H. G., 1950: "A preliminary quantitative analysis of precipitation mechanisms," J. Meteorol., 7, 363-369.

14. Langmuir, I., and K. B. Blodgett, 1946: "A mathematical investigation of water droplet trajectories," U.S.A.A.F. Tech. Rep. No. 5418, 47 pp.

15. Levin, L. M., 1954: "The Coalescence of Charged Cloud Drops", Doklady Akad. Nauk U.S.S.R., 95, 467-470.

16. Lindblad, N. R., and R. G. Semonin, 1963a: Collision efficiency cloud droplets in electric fields. J. Geophys. Res., 68, No. 4, 1051-1957.

17. Lindblad, N. R., and R. G. Semonin, 1963b: Reply to comments by J. D. Sartor concerning collision efficiency of cloud droplets in electric fields. J. Geophys. Res., 68, No. 16.

18. Mason, B. J., 1957: The physics of clouds, Oxford Press, London, p. 201.

19. Moore, C. B., and B. Vonnegut, 1959: Estimates of raindrop collection efficiencies in electrified clouds. Physics of Precipitation, Geophys. Monograph 5, 291-304.

20. Pearcey, T., and G. W. Hill, 1956: A theoretical estimate of collection efficiencies of small droplets. Quart. J. Roy. Meteorol. Soc., 83, 1956.

21. Prokhorov, P. S. 1954, Discussions, Faraday Soc., 18, 41.

22. Proudman, I., and J. R. A. Pearson, 1957: Expansion at small Reynolds number for the flow past a sphere and a circular cylinder. Mech. Fluids. 2, 237-262.

23. Rayleigh, Lord (J. W. Strutt), 1878: Theory of Sound. MacMillan and Co., London, (reprinted Dover 1945), 302 pp.

24. Sartor, D., 1954: "A laboratory investigation of collision efficiencies, coalescence and electrical charging of simulated cloud droplets," J. Meteor., 11, 91-103.

25. Shafrir, U., and M. Neiburger, 1963: Collision efficiencies of two spheres falling in a viscous medium. J. Geophys. Res., 68, No. 13, 4141-4147.